Published in final edited form as:
Neuroimage. 2014 November 1; 101: 96–113. doi:10.1016/j.neuroimage.2014.06.078.

Ictal propagation of high frequency activity is recapitulated in interictal recordings: effective connectivity of epileptogenic networks recorded with intracranial EEG

A. Korzeniewska[1], **M.C. Cervenka**[1], **C.C. Jouny**[1], **J.R. Perilla**[2], **J. Harezlak**[3], **G.K. Bergey**[1], **P.J. Franaszczuk**[1,4], and **N.E. Crone**[1]

[1]Department of Neurology, Johns Hopkins University School of Medicine, 600 N. Wolfe St., Meyer 2-147, Baltimore, MD, 21287, USA

[2]Beckman Institute and Department of Physics, University of Illinois Urbana-Champaign, 405 N. Mathews Ave., Urbana, IL 61801, USA

[3]Department of Biostatistics, Richard M. Fairbanks School of Public Health and School of Medicine Indiana University, 410 W 10th St., Suite 3000, Indianapolis, IN 46202, USA

[4]Human Research and Engineering Directorate, US Army Research Laboratory, 459 Mulberry Point Rd, Aberdeen Proving Ground, MD 21005, USA

Abstract

Seizures are increasingly understood to arise from epileptogenic networks across which ictal activity is propagated and sustained. In patients undergoing invasive monitoring for epilepsy surgery, high frequency oscillations have been observed within the seizure onset zone during both ictal and interictal intervals. We hypothesized that the patterns by which high frequency activity is propagated would help elucidate epileptogenic networks and thereby identify network nodes relevant for surgical planning. Intracranial EEG recordings were analyzed with a multivariate autoregressive modeling technique (short-time direct directed transfer function - SdDTF), based on the concept of Granger causality, to estimate the directionality and intensity of propagation of high frequency activity (70–175 Hz) during ictal and interictal recordings. These analyses revealed prominent divergence and convergence of high frequency activity propagation at sites identified by epileptologists as part of the ictal onset zone. In contrast, relatively little propagation of this activity was observed among the other analyzed sites. This pattern was observed in both subdural and depth electrode recordings of patients with focal ictal onset, but not in patients with a widely distributed ictal onset. In patients with focal ictal onsets, the patterns of propagation recorded during pre-ictal (up to 5 minutes immediately preceding ictal onset) and interictal (more than 24 hours before and after seizures) intervals were very similar to those recorded during seizures. The ability to characterize epileptogenic networks from interictal recordings could have important

Corresponding author: Anna Korzeniewska Ph.D., Department of Neurology, Johns Hopkins University School of Medicine, 600 N. Wolfe St., Meyer 2-147, Baltimore, MD 21287, USA, akorzen@jhmi.edu, Phone: (1) 443 287 7252, Fax: 410 955 0751.

clinical implications for epilepsy surgery planning by reducing the need for prolonged invasive monitoring to record spontaneous seizures.

Keywords

high frequency oscillations (HFOs); seizure onset zone; epileptic network; epilepsy surgery; brain mapping; ECoG

1. Introduction

Recent studies provide growing evidence that epileptogenic networks, rather than a single focal source, contribute to the generation of the ictal state (van Diessen et al., 2013), and that epileptic networks are complex and heterogeneous (Bower et al., 2012). It has been suggested that organization of a neural network in which the “epileptogenic zone” would carry higher “connection weights” than other parts of the network, such as the “irritative zone” or the “symptomatogenic zone” may underlie focal epilepsy and that the variability of seizures, may be due to a variation in the location of the seizure onsets within the larger network (Nair et al., 2004). With the concept of an epileptogenic network, an epileptogenic zone may be defined as a strongly connected network node (or hub), and its successful removal may result in degradation of network activity (Frei et al., 2010). Several studies have demonstrated that network nodes may be identified by network connectivity measures, and that these nodes correspond with the location of resected cortical regions in patients who were seizure-free following surgical intervention (Morgan and Soltesz, 2008; Ortega et al., 2008; Wilke et al., 2011). If accurately identified, disruption or inhibition of these epileptogenic network nodes may be used for prevention or termination of seizures without the need for removal of the entire network, which in turn could lead to more effective medical treatment and better post-treatment outcomes.

Connectivity characteristics of epileptic networks have been found to be frequency-dependent, with high frequency activity most closely correlated with improved postsurgical outcome (Wilke et al., 2011). The role of high frequency activity - HFA (Jiruska and Bragin, 2011; Jiruska et al., 2010; Jouny et al., 2007b; Rodin et al., 2009) or high frequency oscillations - HFOs (Worrell et al., 2008; Worrell et al., 2004) in epilepsy has been extensively investigated recently, and has been reported to be temporally and spatially correlated to the seizure onset zone. During ictal recordings, HFOs were recently observed mostly in the region of seizure onset, and less frequently in areas of secondary spread (Jirsch et al., 2006). The rates and durations of HFOs were significantly higher in the seizure onset zone than outside of it. Moreover, resection of brain regions sampled by intracranial electrodes that recorded ictal HFOs was associated with postsurgical seizure-free outcomes (Fujiwara et al., 2012; Jacobs et al., 2012; Jacobs et al., 2010; Modur et al., 2011; Nariai et al., 2011b; Ochi et al., 2007; Zijlmans et al., 2012).

Furthermore, recent studies suggest that epileptogenic networks exhibit aberrant dynamics not only at the time of seizure onset, but also during interictal seizure-free periods (Bragin et al., 2010; Monto et al., 2007; Zijlmans et al., 2011), and that interictal high frequency activity can also be used to identify the ictal onset zone (Brazdil et al., 2010; Jacobs et al.,

2009; Zijlmans et al., 2009). Interictal activity has been shown to have pathologically strong intrinsic correlations (Monto et al., 2007), and strong coupling in high frequencies (Wilke et al., 2011) among signals recorded near the epileptogenic zone. It has also been shown that despite the apparent discrete localization of the ictal onset zone, epileptic brain networks differ in their global characteristics from non-epileptic brain networks (Horstmann et al., 2010).

Although, high frequency activity appears to be linked to epileptogenesis (Firpi et al., 2007; Jacobs et al., 2008; Rampp and Stefan, 2006; Worrell et al., 2008), its role in seizure generation may depend to a large extent on how it is propagated among sites in cortical networks. Effective connectivity is a particularly promising conceptual framework for understanding this propagation. This concept refers to the pattern of causal interactions between the elements of a network (Friston, 1994; Sporns, 2007). Effective connectivity has been investigated using multivariate measures related to Granger causality (Baccala and Sameshima, 2001; Kaminski and Blinowska, 1991; Sameshima and Baccala, 1999) to study the sources of seizure onset, as well as the neural circuitry of epileptogenic brain tissue (Ding et al., 2007; Franaszczuk and Bergey, 1998; Franaszczuk et al., 1994; Ge et al., 2007; Korzeniewska et al., 2012b; Medvedev and Willoughby, 1999; Takahashi et al., 2007; Wilke et al., 2008; Wilke et al., 2010; Wilke et al., 2009b).

Mapping the propagation of high frequency ictal and interictal activity may provide an important means of defining epileptic networks, in turn contributing crucial information for the selection of brain regions for resective surgery. In particular, understanding of the functional architecture of epileptogenic networks may allow for selective disruption or modulation of key components (nodes or hubs) of these networks to halt seizures without removing the entire network. This approach could potentially improve post-operative seizure control and help prevent post-operative functional deficits. Moreover, if this approach consistently shows a high correspondence between interictal and ictal patterns of effective connectivity, it may be possible to use interictal recordings alone to estimate the epileptogenic zone in patients that would otherwise not be surgery candidates because ictal recordings could not be captured during intracranial monitoring. Finally, this could also reduce the length of stay and the risk of surgical morbidity.

2. Material and methods

2.1. Participants

Data were obtained from six epilepsy patients (3M, 3F, ages 14–50 years, two admissions for Patient #1) with medically resistant partial onset seizures who required implantation of intracranial electrodes for epilepsy surgery planning. The exact placement of electrodes was dictated by clinical necessity alone. The study was approved by the Johns Hopkins Medicine Institutional Review Board, conforming to relevant regulatory standards. Patients were selected with a broad spectrum of seizure patterns with different numbers of available seizure recordings (3–86), different types of arrays (grid and/or depth) and configurations of implanted electrodes, and different underlying pathologies (Table 2). Two of these patients differed from the others in that their ictal patterns were widely distributed at onset. The reasons for this, however, were very different in these two patients and were also reflected in

their post-surgical outcomes. In one, patient #3, the temporal lobes were sparsely sampled with electrode strips, and based on a lateralized ictal onset, the patient underwent a right temporal lobectomy with amygdalohippocampectomy and had pathological confirmation of right mesial temporal sclerosis. This patient had an ILAE 1 outcome at 5 years. This patient's ictal pattern, beginning in several right temporal strip electrodes, was likely captured only after widespread propagation of the seizure. Patient #6, on the other hand, had a large, infiltrating oligodendroglioma involving left frontal and temporal lobes, anterior insula, and anterior hippocampus. She had frequent multifocal interictal epileptiform discharges arising from left frontal, anterior temporal, hippocampal, and basal temporal regions, and thus her epileptogenic zone was likely widely distributed. Several complex partial seizures appeared to arise from a large region that included anterior aspects of the planum temporale and left superior and middle temporal gyri, with rapid spread to left amygdala, anterior temporal tip, and posterior hippocampus. Due to cortical stimulation maps of language and motor function, and concerns that memory function depended on the left hippocampus, only the anterior tip and anterior half of the left superior and middle temporal gyri were resected, understanding that this might only be palliative but would likely avoid harm. The patient's outcome a few months after surgery was ILAE Class 3, and at 4 years it was ILAE Class 5.

2.2. Selection of ictal and interictal intervals

Epileptologists (GKB, MCC) identified the time of seizure onset and electrodes involved (defined as the ictal onset zone) for multiple seizures (3–86) in each patient by visual inspection of the ECoG recordings. Electrographic changes were correlated with clinical seizure semiology based on patient report and review of simultaneously recorded video. Electrographic seizures were defined as rhythmic evolving ictal patterns or low voltage fast activity lasting 10 or more seconds with no accompanying clinical changes (Sanchez Fernandez et al., 2014). Propagation of epileptiform activity was analyzed during ictal, preictal and interictal intervals;

- ictal - 60–260 sec, depending on the seizure duration, recorded immediately after seizure onset,
- preictal - 60–240 sec, depending on the availability of ECoG recordings, recorded immediately before seizure onset,
- interictal (inter-1) - depending on the availability of ECoG recordings (not all interictal segments were saved for review in all patients), 300–500 sec, recorded at least 1 hour before a first seizure, or at least 24 hours before seizure onset and 24 hours after a seizure cessation (visual inspection of ECoG recordings did not revealed any evidence of sleep),
- interictal (inter-2) - depending on the availability of ECoG recordings (not all interictal segments were saved for review in all patients), 300–500 sec, recorded at least 1 hour before seizure onset and 1 hour after seizure cessation (visual inspection of ECoG recordings did not revealed any evidence of postictal slowing or sleep).

Since there is ongoing debate regarding the assumed duration of the postictal period, and some research has shown that a postictal state can persist for 24 hours, we selected two types of interictal epochs for the patients in whom these interictal recordings were available. The interictal epochs were chosen randomly, and we did not limit them to, or exclude any specific patterns e.g. spikes or sharp waves. This was done with a view towards the ease of using the method.

2.3. Implanted electrodes and data recording

Electrode configurations were determined based on results of pre-operative evaluation. Implanted electrodes included only grid electrodes in two patients (Patients #2 and #3), only depth electrodes in one patient (Patient #4), and a combination of grid and depth electrodes in two patients (Patient #5 and #6). One patient (Patient #1) was hospitalized twice and had grid electrodes implanted during the first admission (no resection during the first admission), and a combination of grid and depth electrodes implanted during the second admission (resection performed during the second admission). Electrode positions were determined through co-registration of pre-implantation MRI (Sinai et al., 2005) with post-implantation CT, and cortical gyral anatomy was identified through surface rendering of the pre-implantation MRI and confirmed by comparison to digital photographs taken in the operating room.

Subdural ECoG was filtered with a low-pass 300 Hz analog anti aliasing filter, sampled with 1 kHz sampling rate, and digitally recorded (Stellate system) during interictal, preictal and ictal periods. All recorded ictal and preictal intervals (all patients) were selected for analysis. Interictal recordings were accessible for four patients. All selected recordings were visually inspected, and channels and epochs containing artifact were excluded from further analyses.

2.4. Signal analysis

2.4.1. Matching pursuit (MP) analysis—We computed the time-frequency energy distribution of ictal activity in all recorded channels using a matching pursuit (MP) algorithm (Mallat and Zhang, 1993), which has been previously successfully used for detection of epileptic activity (Jouny et al., 2007a; Jouny et al., 2003), as well as functional activity (Boatman-Reich et al., 2010; Cervenka et al., 2011a; Cervenka et al., 2013a; Cervenka et al., 2013b; Cervenka et al., 2011b). MP is an iterative procedure that decomposes signal $x(t)$ into a linear combination of members of a specified set of functions. In this study we used cosine-modulated Gaussians (Gabor functions), cosines, and Dirac delta functions. Gabor functions provide the best compromise between time and frequency resolution, allowed by the uncertainty principle. Cosines are added to the dictionary for better representation of rhythmic components with constant amplitude, and a Dirac delta is added to represent very short transients (e.g. single spikes). This algorithm performs adaptive approximation of energy density for stationary and non-stationary signals which makes it preferable over alternative short time Fourier transform or wavelet decomposition methods. The MP method is particularly well suited for analysis of rapidly changing signals and is appropriately applied to signals with either linear or non-linear characteristics.

For this analysis, we expanded the frequency range (70–175 Hz) we analyzed in our preliminary study (Korzeniewska et al., 2009), and the raw recordings were band-pass filtered into three bands of high frequency activity 70–115 Hz, 125–175 Hz, and 185–235 Hz (to avoid power line artifact at 60 Hz and its harmonics 120 Hz, 180 Hz, and 240 Hz), and a lower frequency band (0–40 Hz). We did not observe significant energy components above 180 Hz in analyzed signals likely due to characteristics of our recordings (1 kHz sampling rate, 300 Hz low-pass analog anti-aliasing filter). Electrode sites with increased energy of the high frequency components (70–115 Hz and 125–175 Hz) of ictal signals were selected for further SdDTF analyses, due to requirement of multivariate autoregressive model (MVAR), as described below.

2.4.2. Short-time direct directed transfer function (SdDTF) analysis—Short-time direct Directed Transfer Function (SdDTF) (Korzeniewska et al., 2008) has been based on the concept of Granger causality, where one can consider an observed time series *x(t)* to have a Granger-causal, or G-causal, effect on another time series *y(t)*, if knowledge of *x(t)*'s past significantly improves prediction of *y(t)* (Granger, 1969). SdDTF applies a multivariate autoregressive model (MVAR), which uses past observations in recorded signals to describe current values in these signals, and gives an estimate of the direction and intensity of interactions between recording sites as a function of frequency. SdDTF measures only direct G-causal interactions, not confounded by indirect interactions (mediated by other sites) (Korzeniewska et al., 2008; Korzeniewska et al., 2003). To meet MVAR requirement of signals stationarity for highly dynamic ictal signals we applied an algorithm introduced by Ding et al. (Ding et al., 2000), which enables calculation of SdDTF in short windows shifted in time, when multiple realizations of the same stochastic process are available. Seizures originating from the same epileptogenic zone often produce very similar EEG signals, particularly if they are recorded intracranially (grids, strip or depth electrodes) (Jouny et al., 2007a). Multiple seizures from the same patient, therefore, may often be treated as repeated realizations of the same stochastic process which is stationary over short periods.

MVAR requirement of signal stationarity states a natural trade-off between the length of the shifting window and the number of analyzed channels, as described in Korzeniewska et al., 2008. Therefore, we selected signals based on their power augmentation, indicated by matching pursuit (MP), as described above. The selected signals of multiple recordings (of ictal, preictal, or interictal intervals), band-pass filtered (70–115 Hz, 125–175 Hz) and downsampled (to 500 Hz), were normalized over time by subtracting their mean and dividing by their standard deviation in each channel, and in each window (Korzeniewska et al., 2008). For each set of multiple recordings, a common MVAR-model order was determined using Akaike information criterion (AIC). The coefficients were calculated by solving the Yule Walker equations, with estimates of cross-correlation matrices based on all available seizures (or similar number of interictal epochs), using the Levinson-Wiggins-Robinson algorithm. Windows used for estimation varied from 50 msec to 3 sec for different patients, depending on the number of available seizures (shorter when larger number of seizures was available). Windows were shifted by 50–500 msec depending on window length. To illustrate connectivity patterns, the SdDTF values were integrated over analyzed frequency bands and time intervals. The average of all SdDTF values representing directed

flows originating in an electrode site (outflows), as well as the average of all SdDTFs values representing directed flows ending in a given electrode site (inflows), were calculated. To compare between subjects and different frequency ranges, the values of averaged outflows (divergence) and inflows (convergence) were normalized (for each patient, each frequency band, and each inter-, pre- and ictal epoch) to the interval (0,1) with 0 indicating minimum, and 1 indicating maximum value.Sites indicated by SdDTF analyses as most active nodes of the epileptogenic network were compared to the ictal onset zones identified by epileptologists (GKB, MCC).

2.5 Statistical analysis

Mixed effects logistic models (Molenberghs, 2005) were used to compare the percentages of electrodes revealing ictal activity. In particular, we were modeling the odds ratios of the activity detected using the three frequency bands: 0–40Hz, 70–115Hz and 125–175Hz. Odds ratio is defined as the ratio of odds of detection of ictal activity occurring in one frequency band to the odds in another frequency band, which means the ratio of the probability of ictal increase in energy of 70–115 Hz activity to the probability of lack of the ictal increase in energy of 70–115 Hz activity, divided by to the ratio of the probability of ictal increase in energy of 0–40 Hz activity to the probability of lack of the ictal increase in energy of 0–40 Hz activity, and similarly for 125–175 Hz. Mixed effects modeling is necessary since the electrode responses are correlated within each patient.

The two-sided Fisher's Exact Test for binary data was used to compare the proportions of electrodes detected using high frequency detections method which were either overlapping and non-overlapping with the clinical evaluations (Blaker, 2000; Fisher, 1935).

3. Results

3.1. High and lower frequency ictal activity vs. seizure onset zone

High frequency ictal activity (70–175 Hz) was observed within the ictal onset zone and its vicinity, while the lower frequency ictal activity (0–40 Hz) occurred more broadly (as identified by matching pursuit (MP) analysis, and statistically compared to the preictal interval). In some cases, e.g. Patient #1 and Patient #2, prominent increases in energy of the lower frequency ictal activity were observed at all recorded sites, while increases in energy of the high frequency component of ictal activity were observed only for signals recorded in the vicinity of the ictal onset zone (Patient #1 - Figs. 1, 2).

Figure 1 shows the energy density in the time-frequency domain, for lower (0–40 Hz, left panel), and high frequency (70–120 Hz, right panel) components of ictal activity at several recording sites. Figure 2 shows reconstructions of the implanted electrodes and an axial T2-weighted image depicting a left mesial occipital lesion identified on pre-operative MRI (bottom-right). As shown in Figs. 1 and 2, increases in energy of high frequency ictal activity occurred in close proximity to the lesion identified by MRI (left posterior mesial occipital - marked by red arrow in Fig. 2);

- within the seizure onset zone (LPD1-LPD5, LSP1-LSP5) as identified by epileptologists,

- in the adjacent grid electrodes LOG19-LOG21 located over the left temporo-parieto-occipital junction (lateral to the lesion),
- in the adjacent strip electrodes LSP1-LSP4 over the left precuneus (superior to the lesion), and
- in the depth contacts LPD2-LPD5 (passing through the left posterior mesial occipital region within the lesion area).

The number of electrodes revealing high frequency ictal activity (70–115 Hz and 125–175 Hz) was smaller than the number of electrodes revealing lower frequency ictal activity (0–40 Hz) for all patients with focal ictal onsets (but not Patients #3 and #6, who had widely distributed ictal onsets). Another exception to this rule was the larger number of electrodes in the 125–175 Hz range in Patient #4, who had only depth electrodes implanted). Table 1 lists the number of electrodes revealing significant increases in energy of ictal activity, as compared to energy of preictal activity (T-test with FDR correction for multiple comparisons), for frequency ranges 0–40 Hz, 75–115 Hz, and 125–175 Hz for each patient diagnosed with focal epilepsy. Increases in energy of ictal activity were observed in all electrodes identified by clinicians as sampling the seizure onset zone, in all frequency ranges.

Using mixed effects logistic models, which takes into account the correlations within patients, and treating the percentage of electrodes revealing ictal activity as a response, we showed that significantly fewer electrodes demonstrated an increase in energy in the 70–115 Hz or 125–175 Hz range compared to the 0–40 Hz range. Estimated odds ratios are: 0.17 (p-value < 0.0001) for 70–115 Hz vs. 0–40 Hz, and 0.23 (p-value < 0.0001) for 125–175 Hz vs. 0–40 Hz, which means that the estimated probability of observing an increase in energy of 0–40 Hz activity are about 5.8 times higher (1/0.17) than for 70–115 Hz, and about 4.4 (1/0.23) times higher than for 125–175 Hz.

3.2. Propagation of high and lower frequency ictal activity vs seizure onset zone

In focal epilepsy, by definition, ictal activity originates in the seizure onset zone, and propagates from the source, spreading over a larger area. Effective connectivity revealed by SdDTF was not always characterized by such a pattern of propagation for the lower frequency component. The left panel of Figure 3 shows the evolution of seizures for Patient #2, diagnosed with temporal lobe epilepsy. Arrows represent SdDTF integrated over frequency (0–25 Hz) and time (periods of 1 second). Prominent propagation was observed mostly in the vicinity of the onset zone, not only from the sites (RPT2-RPT6) identified by clinicians. This suggests that in some patients, lower frequency ictal activity may not be a precise indicator of the seizure onset zone.

Whereas propagation of the lower frequency component of ictal activity may be nonspecific in some cases, propagation of the high frequency component of ictal activity appeared to be more indicative of the seizure onset zone. When electrode sites were selected on the basis of increases in energy (MP) of the high frequency component of epileptic activity, and SdDTF was calculated for high frequency activity (70–115 Hz, right panel of Fig. 3), the propagation of high frequency activity revealed the location of the ictal onset zone (RPT2-

RPT6) as determined by epileptologists. The most prominent propagations were outgoing from the onset zone. Propagations of high frequency activity incoming into the onset zone were also present, but were weaker. Moreover, these outflows and inflows of high frequency activity occurred continuously during the whole ictal epoch, as well as during the pre-ictal epoch. A very similar pattern of ictal outflows and inflows was also obtained for the frequency range 125–175 Hz.

Similarly, as a change in signal energy of high frequency ictal activity was a better indicator of the seizure onset zone than a change in signal energy of lower frequency ictal activity, the propagation of high frequency ictal activity appeared to be a better indicator of the seizure onset zone than the propagation of lower frequency ictal activity (discussed further in and illustrated in 3.5. - Figs. 8 and 9).

3.3. Ictal high frequency effective connectivity

Because of the observed persistence of high frequency inflows and outflows during the whole ictal epoch and during preictal epochs, we averaged the magnitudes of the outflows and inflows over ictal and preictal periods separately, yielding a measure of the overall divergence (averaged outflows) and convergence (averaged inflows) of activity propagation. Figure 4 illustrates the average inflows and average outflows observed in Patient #2 for two high frequency ranges of 70–115 Hz and 125–175 Hz. The highest values of averaged outflows and averaged inflows for both frequency bands and both periods have been observed at RPT2, which was identified by epileptologists as the seizure onset zone. In all other patients diagnosed with focal epilepsy (Fig. 4, 6, 7, 8, 10), we have also observed a similar pattern of continuous high frequency inflows and outflows that preferentially involved the ictal onset zone. Even for a patient with widely distributed ictal onset (Patient #3, Fig. 5), persistent divergence/convergence was observed, however there was no obvious dominance or stability in the sites with greatest outflows or inflows. The highest values of averaged outflows and averaged inflows have been observed at site RBT3 (red arrows). In this patient, a right temporal lobectomy included resection of RBT3, and the patient has remained seizure-free for five years.

3.4. Interictal high frequency effective connectivity

Persistent inflows and outflows of high frequency activity were also observed during interictal periods. For Patient #4 (Fig. 6), with depth electrodes, we found the same pattern of prominent outflows and inflows involving the seizure onset zone (RA2-RA3), for interictal epochs (inter-2; recorded at least 1 hour before and 1 hour after seizure onset), as for ictal and preictal epochs.

Analyses of two types of interictal epochs (inter-2; recorded at least 1 hour before the first seizure, and inter-1; recorded at least 24 hours before and 24 hours after a seizure) revealed very high similarity in patterns of the average outgoing and incoming propagations for both types of the interictal epochs, as well as for pre- and ictal epochs (Patient #5, Fig. 7). Sites DPB6-DPB8 were identified as the ictal onset zone by epileptologists (GKB, MCC), and as shown in Fig. 7, grid contacts LGD20, and LGD27-LGD28 were located immediately

adjacent to the depth contacts DPB7-DPB8. This patient has remained seizure-free for 4 years following resection.

A similar consistency of average high frequency propagation across inter-, pre- and ictal epochs, was also observed for Patient #1 (Fig. 8, 10).

3.5. Effective connectivity vs configuration of implanted electrodes

Patient #1 underwent intracranial monitoring twice (Figs. 2, 8, and 10) and provided a unique opportunity to investigate the ictal onset zone with two different sets of implanted electrodes. The two monitoring evaluations were 6 months apart. During the first admission, the patient was implanted with grid and strip electrodes covering mostly left anterior brain areas, with a single strip sampling the occipital region (LOS1-LOS8), ultimately identified by the epilepsy team as sampling the region closest to the ictal onset zone (Fig. 8). During the second admission, grid electrodes were implanted over left posterior regions, and depth electrodes were implanted in a region of cortical dysplasia revealed by MRI (Fig. 2).

SdDTF analysis of propagation of high frequency activity recorded during the **first admission** (Fig. 8) revealed a stable pattern of outflows and inflows involving LOS3 (left occipital region) during all tested intervals; ictal, preictal, and interictal (inter-1 and inter-2). This site was among the electrodes (LOS2-LOS6) identified by clinicians as the ictal onset zone. Similarly, as described in 3.2., lower frequency activity (Fig. 9) was less specific in this case and indicated more sites: LFPG12, LPTS3, LOS2, and LOS8. However, only one of these (LOS2) was located within the ictal onset zone. LOS8 was in close proximity, superficial to LOS2 and LOS3, but LPTS3 and LFPG12 were rather distant from the onset zone (left prefrontal cortex).

Figure 10 shows the results of high frequency analysis for recordings from the **second admission** of Patient #1. The site LPD3 indicated by SdDTF analysis was located within the LPD2-LPD5 region, identified as the ictal onset zone by clinicians. Lower frequency SdDTF analyses (Fig. 11) indicated sites LPD3 and neighboring LAD2, located posteriorly.

It is noteworthy that both high frequency analyses of the two intracranial monitoring sessions of Patient #1 indicated electrodes closest to the ictal onset zone identified by clinicians. For the **first admission**, SdDTF indicated the site LOS3 (Fig. 8), which is the closest electrode to the medial occipital lesion that was targeted during the recording session. During the **second admission**, SdDTF indicated the site LPD3 (Figs. 2 and 10), which is within the region of cortical dysplasia identified as the seizure onset zone (Fig. 2). Lower frequency analyses were not as consistent. The resection included the mesial occipital lesion and the patient had a single seizure post-operatively after missing medication but has had no additional seizures in the 3 years following surgery.

3.6. Effective connectivity in epilepsy with widely distributed ictal onset

Patient #6 had an infiltrating left temporal tumor with indistinct borders on MRI (Fig. 12). Similar to Patient #3, who had seizures with widely distributed ictal onset, there was no clear dominance or temporal stability in the sites with greatest outflows and/or inflows (Fig.

12). However, the ictal onset zone identified by epileptologists was also widely distributed (LFG33-LFG36 and LFG41-LFG43) (Fig. 12).

3.7. Quantitative representations of epileptic effective connectivity

Table 2 lists the recording sites identified as the ictal onset zone by epileptologists vs. those identified by SdDTF analysis of propagation of high frequency activity for each patient.

A quantitative summary of our results is illustrated in Fig. 13 and Fig. 14. For each electrode site, the average magnitudes of inflows and outflows (depicted with purple and green colors in Figs. 4, 6, 7, 8, 10), were summed and transformed into an interval value (0,1), where 0 represents minimal value, and 1 represents maximal value. A mean value of the transformed averaged flows (MTAF) and its standard error, calculated over both inflows and outflows, over both high frequency bands (70–115 Hz and 125–175 Hz), and over interictal, preictal, and ictal periods, for each patient, are shown in Figure 13. Large values of MTAF indicate large flows, both from *and* to the recording site. Small values of standard error of MTAF indicate low variability of this measure over inter-, pre-, and ictal epochs. In each patient with focal epilepsy (Patients #1, #2, #4, #5), sites with MTAF values greater than 0.8 and of low standard error were among the sites identified by clinicians to comprise the ictal onset zone (Table 2). As mentioned in 3.4., in Patient #5 grid contacts LGD27-LGD28 and LGD20 were located immediately adjacent to the depth contacts DPB7-DPB8. For LGD27 and LGD28 MTAF>0.8, and for LGD20 MTAF value was slightly lower than 0.8. For patients with widely distributed ictal onset (Patients #3, #6), the values of MTAF were smaller than 0.8.

Table 3 lists the number of electrodes within the seizure onset zone as identified by epileptologists, and as indicated by MTAF values greater than the 0.8 threshold. Only for Patient #5, for whom grid contacts LGD27-LGD28 were located immediately adjacent to the depth contacts DPB7-DPB8, the two grid contacts (LGD27-LGD28) did not overlap with the onset electrodes identified by epileptologists. For all other patients with focal ictal onsets, the electrodes indicated by MTAF>0.8 sampled the seizure onset zone identified by epileptologists.

We tested the detection of sites by MTAF>0.8, which were either overlapping or non-overlapping with the sites identified by epileptologists. Since the detection based on MTAF>0.8 was performed in the same patient, we treated the data as paired binary data with the two outcomes defined as detection and non-detection. Thus, there were 4 possible outcome combinations consisting of detection and non-detection of overlapping and non-overlapping electrodes. The data in Table 3 indicate that for all five patients at least one overlapping electrode was detected. However, only for 1 patient, the detection was seen in the non-overlapping region. Using the two-sided Fisher's Exact Test for binary data, we rejected the hypothesis that sites indicated by high frequency activity were non-overlapping with sites identified by epileptologists as the ictal onset zone (p-value = 0.048).

It is worth noting that the distributions of MTAF values can be different (e.g. flatter, sharper, bi-modal, etc.) for different patients (Fig. 13). Because of this, we chose sites with the highest and least variable combined index of high frequency inflows and outflows

(MTAF>0.8) to illustrate the results of our method in relation to the seizure onset zone identified by clinicians. Although we thought these provisional criteria worked quite well, MTAF provides a continuous measure that clinicians can use to estimate the relative contribution of sites to ictogenesis and prioritize sites for resection. Such prioritization may be particularly useful when sites in the seizure onset zone overlap or are near eloquent cortex. Nevertheless, further study on a population of patients with resections limited to sites chosen by our criteria, including postsurgical outcomes for these patients, would be needed to determine whether these criteria are sufficient to ensure seizure freedom.

Figure 14 shows MTAF values calculated only for interictal periods (for patients for whom interictal data were available, i.e. Patients #1, #4, #5, and #6). For patients with focal ictal onsets, the results for interictal epochs were very similar to those obtained with all epochs, including ictal epochs (Fig. 13). Interestingly, in Patient #5 the grid electrodes (LGD27-LGD28, and LGD20) immediately adjacent to the depth contacts DPB7-DPB8, identified as the onset zone, had MTAF>0.8 for interictal epoch inter-2 (Fig. 14), and had MTAF< 0.8 for interictal epoch inter-1, however still higher than MTAF values for the other investigated electrodes. While, the depth contacts DPB7-DPB8 identified as onset zone had MTAF>0.8 for both interictal epoch inter-1and inter-2. Similarly, in Patient #1 (second admission) the depth contacts LPD1 and LAD2 immediately adjacent to LPD3, identified as the ictal onset zone (Fig. 2), had MTAF>0.8 for interictal epoch inter-2, and had MTAF< 0.8 for interictal epoch inter-1. This would suggest stronger connectivity in these very local networks, as far as an hour before the seizure onset. In Patient #6 with widely distributed ictal onset, MTAF values calculated for interictal periods showed less consistency with MTAF values averaged over interictal, preictal and ictal periods. For this patient, MTAF analysis for epoch inter-2 would suggest onset close to the site LFG47, and for epoch inter-1 would suggest onset close to the site LFG37 (immediately adjacent to the resected LFG36). However, the majority of inter-1 epochs were recorded before the first seizure, while majority of inter-2 epochs were later during admission, and our findings may have been influenced by changing doses of antiepileptic medications during monitoring. LFG37 was found on electrocortical stimulation mapping to be immediately adjacent to motor cortex and LFG47 was found to be over language cortex, therefore these regions were not resected. The patient continued to have simple partial seizures 1–2 times per day 2 months post-operatively.

In summary

- Increases in energy of the high frequency component (70–175 Hz) of ictal activity were limited to the ictal onset zone and its vicinity, while increases in energy of the lower frequency ictal activity (0–40 Hz) were often observed more broadly (in some cases in all recorded sites). However, this observation did not hold in patients #3 and #6, who had widely distributed ictal onsets.
- Propagation of high frequency activity (70–175 Hz) was consistent with the location of the ictal onset zone as identified by clinicians, while prominent propagation of lower frequency ictal activity (0–40 Hz) was also observed in the vicinity of the ictal onset zone, but not in the onset zone alone.

- Persistence of inflows and outflows (divergence/convergence) of high frequency activity was a good indicator of the seizure onset zone.
- The divergent/convergent “architecture” of epileptogenic networks was also observed during interictal periods.
- For one patient who was hospitalized twice with different configurations of implanted electrodes, the divergence/convergence of high frequency activity (70–175 Hz) indicated electrodes closest to the ictal onset zone during both admissions.
- Seizures in patients with widely distributed ictal onset were not characterized by a clear dominance or temporal stability in the sites with greatest divergence/convergence (the ictal onset zone identified by epileptologists was also widely distributed).
- In patients diagnosed with focal epilepsy, the highest mean value of the transformed averaged flows (MTAF) - a measure of divergence/convergence - indicated the same sites when applied to ictal and interictal recordings.

4. Discussion

4.1. High frequency connectivity among epileptogenic networks

In acquired epilepsies, structural or metabolic disturbances are believed to reorganize neuronal circuitry in a manner that enhances synchronization (Engel Jr., 2012). The intrinsic organization of local cortical circuits likely determines their excitability and synchronization, and thus their unique predisposition to generate ictal activity, which may also be mediated by broader networks. It has been recently reported that the activity of epileptogenic networks, rather than a single focal source, contributes to the generation of the ictal state (van Diessen et al., 2013), and that the network organization within the epileptogenic zone carries higher “connection weights” than other parts of the cerebral network (Nair et al., 2004). Several structural, molecular, and functional changes have been found within epileptogenic neuronal networks. These include decreased afferent input, sprouting of axon collaterals and formation of autapses, local alteration of inhibition, increased density of NMDA or/and AMPA receptors, and changes in intrinsic neuronal properties due to various acquired channelopathies (Dudek and Sutula, 2007; Engel Jr., 2012; Yaari and Beck, 2002). These changes have the potential to increase neuronal excitability among interconnected neuronal clusters, and to cause a chain reaction via divergent excitatory connections, which forces surrounding neurons to also generate action potentials (Traub and Wong, 1982), and may further contribute to altered network synchronization (Jiruska and Bragin, 2011).

On the other hand, it has been shown that there is a sharp delineation between areas showing intense hypersynchronous firing indicative of recruitment during seizures, and adjacent territories, in which established ictal discharges may fail to invade, even though the synaptic bombardment of these areas is extremely intense (Schevon et al., 2012). Therefore, it is highly reasonable to investigate causal interactions, or effective connectivity, among the

components of an epileptogenic network to identify nodal points responsible for the transformation of local pathological activity into global patterns as seizures.

It has been demonstrated in humans, that high frequency activity (HFA) is generated locally by clusters of spatially separated neurons diffusely distributed in the epileptic tissue (Jiruska and Bragin, 2011). The high frequency activity is thought to reflect hypersynchronized action potentials within small discrete neuronal clusters, facilitating synaptic transmission through local networks (Bragin et al., 2010), or to reflect inhibitory field potentials, which facilitate information transfer by synchronizing neuronal activity over long distances (Engel et al., 2009). The high frequency activity is generated in local clusters of neurons that are spatially stable over time. With reduced inhibitory influences, however, these clusters may increase in size, coalesce, synchronize, and the activity may propagate (Engel Jr., 2012). When the synchrony of discharges between pathologically interconnected neuronal clusters reaches a certain level, it manifests as a seizure (Jiruska and Bragin, 2011).

There are increasing numbers of studies pointing to the importance of high frequency activity - HFA (Jiruska and Bragin, 2011; Jiruska et al., 2010; Jouny et al., 2007b; Rodin et al., 2009), or high frequency oscillations (HFOs) (Burns et al., 2012; Firpi et al., 2007; Jacobs et al., 2008; Jacobs et al., 2010; Jirsch et al., 2006; Nariai et al., 2011a; Ochi et al., 2007; Rampp and Stefan, 2006; Worrell et al., 2008; Worrell et al., 2004), for localizing the seizure onset zone. Recent studies have reported increased postsurgical seizure-free outcomes after resection of brain regions revealing ictal HFOs (Fujiwara et al., 2012; Jacobs et al., 2012; Jacobs et al., 2010; Modur et al., 2011; Nariai et al., 2011b; Ochi et al., 2007; Zijlmans et al., 2012). However, the frequency ranges of the reported HFOs vary between studies (Bragin et al., 2010; Firpi et al., 2007; Jirsch et al., 2006; Rampp and Stefan, 2006; Worrell et al., 2004; Zijlmans et al., 2011). It has been observed that highly synchronized high frequency activity (HFA) remains confined to the same, possibly epileptogenic, area during interictal and ictal periods (Nariai et al., 2011b; Wilke et al., 2011; Zijlmans et al., 2011). It has also been reported that repeated activation of interneurons can cause a decrement in the inhibitory response and, therefore, enhanced excitability (Engel Jr., 2012), and that the occurrence of high frequency activity over a long time period may cause a modification of synaptic transmission and increase the chances of triggering seizures and propagating epileptic activity (Jiruska and Bragin, 2011). Thus, ictogenesis may fundamentally depend on altered or abnormal connectivity within the networks that comprise the epileptogenic zone.

Altered functional connectivity has been reported in epilepsy patients in a variety of frequency ranges. Some researchers have reported that epilepsy patients have a significantly higher index of interictal functional connectivity in theta frequencies than do non-epilepsy patients (Douw et al., 2010a), and this increased theta connectivity is related to the cumulative number of seizures (Douw et al., 2010b). Other studies have shown rich alpha band connectivity with a clear modular structure across interictal networks (Chavez et al., 2010); increased local alpha and beta connectivity with reduced connectivity with distant areas (Uhlhaas and Singer, 2006); and increased alpha, beta, and gamma interictal interdependencies, with reinforced functional connectivity among networks of neuronal assemblies constituting the epileptogenic zone (Bettus et al., 2008). Studies have also shown

lower functional connectivity between seizure generating areas and other brain regions for frequencies below 75 Hz, but not for high frequencies 75–500 Hz (Warren et al., 2010). Our study finds increased divergence/convergence of high frequency (70–175 Hz) propagation within the seizure onset zone identified by clinicians. On the other hand, divergence/convergence of lower frequency (0–40 Hz) propagation may (Fig. 11 - for comparison Fig. 10), or may not (Fig. 9 - for comparison Fig. 8), overlap with the seizure onset zone in the same patient (Patient #1), depending on the configuration of electrodes used (Fig. 11 - second admission vs. Fig. 9 - first admission). Thus, measures of propagation at high frequencies appear, in our study, to be more accurate in identifying the altered or abnormal "architecture" of epileptogenic networks.

4.2. SdDTF as a measure of high frequency ictal/interictal effective connectivity

It has been previously shown that the direction of ictal activity propagation is able to provide information regarding localization of the epileptogenic zone, by the simultaneous analysis of multiple EEG channels (Baccala et al., 2004; Franaszczuk and Bergey, 1998; Franaszczuk et al., 1994; Ge et al., 2007; Jung et al., 2011; Lu et al., 2012; Medvedev and Willoughby, 1999; Mullen et al., 2011; van Mierlo et al., 2013; van Mierlo et al., 2011; Varotto et al., 2012b; Wilke et al., 2008; Wilke et al., 2009a, 2010; Wilke et al., 2009b). It was also recently shown that propagation of high frequency activity (>80 Hz) can be observed in the preictal interval (3 sec before the clinically recognized ictal onset) (Adhikari et al., 2013). However, no previous studies that we are aware of have investigated propagation of high frequency ictal and interictal activity.

Using time-frequency energy analysis (MP) of ictal recordings, we confirmed that high frequency energy (70–175 Hz) is significantly increased within the seizure onset zone, compared to the preictal interval. Among these sites, we investigated the propagation of high frequency activity using the short time direct directed function (SdDTF).

In all patients analyzed for propagation of high frequency activity, SdDTF analysis indicated sites within the seizure onset zone determined by epileptologists (Table 2). From 10–21 sites indicated by MP analysis as sites with the highest ictal increase of high frequency activity, the SdDTF analysis of high frequency propagations narrowed the "suspected" zones to one or two recording loci. When depth and grid contacts were in close proximity (Patient #5, Fig. 7), SdDTF analysis of high frequency activity narrowed the suspected zones to five of the closely neighboring recordings sites. Thus, the effective connectivity of epileptogenic networks measured by the propagation of high frequency activity appeared to yield more specific information about the location of the seizure onset zone, than increases in energy of high frequency activity alone.

In some patients SdDTF indicated fewer sites than those identified by clinicians, potentially identifying a more discrete ictal onset zone (Table 2). Other studies have also identified more discrete loci for frequencies up to 80 Hz, using methods similar to SdDTF, as compared to clinical evaluation (Jung et al., 2011; Lu et al., 2012; Mullen et al., 2011; van Mierlo et al., 2013; van Mierlo et al., 2011; Varotto et al., 2012a; Varotto et al., 2012b; Wilke et al., 2009a, 2010). Ictal onset zones identified clinically may have been broader when the initial patterns of seizure propagation were not evident from visual analysis but

appeared to begin simultaneously at multiple sites. In our study, propagation of high frequency epileptic activity appeared to be a good indicator of the seizure onset zone, showing nodes of divergence/convergence within the area identified by clinicians, and even limiting the number of "suspected" loci. In contrast, prominent propagation of lower frequency ictal activity (0–40 Hz) was observed in the vicinity of the ictal onset zone, but not in the onset zone alone. Thus, high frequency propagation measured by SdDTF could potentially be helpful in planning epilepsy surgery, particularly when the onset zone is within or near eloquent cortex that would limit the extent of the planned surgical resection.

The mean value of the transformed averaged flows (MTAF) and its standard error, introduced in this study, provides a useful measure of the overall intensity and stability of the propagation of high frequency ictal and interictal activity for individual recording sites. By providing a combined measure of the divergence and convergence of propagation involving any given site, MTAF may help indicate nodes of epileptogenic networks.

Moreover, SdDTF, which is derived from a multi-channel model of network interactions, indicated sites within the seizure onset zone determined by epileptologists reviewing electrographic changes in single channels (in conjunction with clinical seizure onset based on video review and patient report). This supports the concept of an epileptogenic network with higher connection weights among network nodes, rather than a single focal source (Frei et al., 2010; Nair et al., 2004; van Diessen et al., 2013). This is in agreement with other studies, which have shown that epileptic nodes may be indicated by network connectivity measures (Morgan and Soltesz, 2008; Ortega et al., 2008; Wilke et al., 2011).

4.3. Interictal high frequency effective connectivity

During intracranial monitoring, patients may have a small number of seizures in spite of medication withdrawal, and this limited sample may not fully represent their habitual seizures or disclose the entirety of the epleptogenic zone. Furthermore, infrequent seizures can prolong monitoring, increasing the risk of complications, particularly surgical infections. In these circumstances, estimation of the epileptogenic zone from interictal recordings alone could potentially have a profound clinical impact.

HFOs are reported to remain confined to the epileptogenic area during ictal, as well as interictal periods (Brazdil et al., 2010; Jacobs et al., 2009; Monto et al., 2007; Zijlmans et al., 2011; Zijlmans et al., 2009). Interictal high frequency oscillations (HFOs) are believed to be markers that reflect the primary neuronal disturbance responsible for seizure origination (Bragin et al., 2010), and to be more accurate markers of epileptogenicity than spikes (Jacobs et al., 2010; Perucca et al., 2014). In this study, however, because we used band-pass (70–175 Hz) filtered signals of randomly chosen interictal intervals, and we did not limit them to, or exclude any specific patterns, e.g. spikes or sharp waves, the influence of both HFOs and spikes could have been included in the measured propagation of high frequency activity.

It has been observed that neuronal clusters among epileptogenic network may be hypersynchronous (Engel Jr., 2012), and that interictal connectivity in epileptic patients is different than in non-epileptic subjects (Bettus et al., 2008; Chavez et al., 2010; Douw et al.,

2010a; Douw et al., 2010b; Uhlhaas and Singer, 2006; Warren et al., 2010). These findings support the concept of epileptogenic networks (van Diessen et al., 2013), with higher connection weights within the epileptogenic zone (Nair et al., 2004). Thus, ictogenesis may fundamentally depend on altered or abnormal connectivity within the networks that comprise the epileptogenic zone, and analyses of the interictal effective connectivity of networks underlying the propagation of high frequency activity may provide a means for detecting this abnormal connectivity.

Our analyses revealed that high frequency effective connectivity in epileptogenic networks is very stable in terms of outflows from, and inflows into, the ictal onset zone during inter-, pre-, ictal, and postictal intervals (Figs. 6, 7, 8, 10). For all patients in whom interictal recordings were available, our SdDTF analyses of interictal recordings indicated majority of the same sites during ictal and preictal epochs. These results are in agreement with previous studies employing adaptive directed transfer function (ADTF) to interictal spike recordings (Wilke et al., 2009a). The persistence of large high frequency propagations from the onset zone to all other analyzed sites, and from all other sites to the onset zone, during inter-, pre-, ictal, and postictal epochs, suggests that the epileptogenic zone is the node of a stable epileptogenic network. A similar concept of epileptogenic network nodes has been proposed as the result of between-ness centrality analyses (Wilke et al., 2011), which have suggested the importance of these nodes in the propagation of activity across a network.

4.4. High frequency connectivity in epilepsy with widely distributed ictal onset

Patterns of high frequency activity flow observed in patients with widely distributed ictal onset, differed from patterns observed in patients diagnosed with focal epilepsy. The variability of the mean value of the transformed averaged flows (MTAF) was relatively large for all channels in these patients. In one patient (Patient #3), multiple sites were identified by epileptologists as the ictal onset zone, however, the highest MTAF value, albeit lower than 0.8, occurred at one electrode, suggesting it as a node for high frequency activity propagation. The variance in this site was larger than for patients with focal ictal onsets. A right anterior temporal lobectomy was performed (pathology - mesial temporal sclerosis), including resection of the region containing the electrode, and the patient has remained seizure-free for 5 years. In this instance, high frequency connectivity measures identified a more discrete ictal onset zone compared to clinical evaluation of ECoG signals with good surgical outcome when the area was resected.

One patient (Patient #6) with a very extensive infiltrating tumor, also had a very broad seizure onset based on clinical interpretation. The pattern of high frequency activity propagation also indicated an extensive ictal onset zone. The largest outflows and inflows of high frequency activity were observed for sites within the ictal onset zone and the pattern of MTAFs (Fig. 13) was clearly distinguishable from patterns obtained for patients with focal ictal onsets. None of the values of MTAF were larger than the 0.8 threshold, suggesting that none of the recording sites were a dominant node of the epileptogenic network, and confirming the diagnostic impression that the seizure onset zone was widely distributed. Interestingly, the pattern of MTAFs for interictal epochs in this patient was more similar to MTAFs observed in patients with focal ictal onsets, suggesting a single site as the ictal onset

zone. The patient underwent a left anterior temporal lesionectomy of an oligodendroglioma, including regions identified by epileptologists as the ictal onset zone, however, sparing the site suggested by the pattern of MTAFs for interictal epochs because it was found to be positioned over eloquent cortex. The patient continued to have seizures post-operatively.

Overall, for all patients studied in this diverse group, the seizure onset zones indicated by propagation of high frequency activity, during ictal, preictal and interictal periods, were located within regions identified by epileptologists to be the ictal onset zones. For one patient, in addition to sites within the epileptogenic zone identified by epileptologists, SdDTF analysis indicated three additional electrode sites in the immediate vicinity. These sites also happened to be included in the patient's surgical resection. This patient has remained seizure-free 4 years post-operatively. In fact, all patients are currently seizure-free post-operatively, excluding the patient with a large dominant temporal oligodendoglioma in whom MTAF analysis indicated sites not ultimately resected because they were located over eloquent cortex.

SdDTF analysis of interictal high frequency activity appears to reliably estimate the ictal onset zone. This could have great clinical implications. Patients who would otherwise not qualify for surgical intervention because too few seizures were captured during long-term monitoring with intracranial electrodes, may be able to proceed with surgery based on analyses of interictal intracranial recordings using these techniques.

Our study supports the concept of epileptogenic networks (van Diessen et al., 2013), and higher connectivity within the epileptogenic zone (Nair et al., 2004). However, it is unknown whether networks and network nodes responsible for seizure propagation are similar to networks responsible for normal physiological functions. We have observed a divergence of functional high frequency activity (70–115 Hz) during speech production (Korzeniewska et al., 2011) as well as a convergence of high frequency activity immediately preceding spoken responses (Korzeniewska et al., 2012a). Thus, the phenomena of convergence and divergence are not exclusive to epileptic networks. However, in our studies of speech production, we have not observed convergence and divergence occurring simultaneously in the same node. This characteristic could potentially be unique to epileptogenic networks, perhaps revealing positive feedback loops within the epileptogenic zone and between it and surrounding regions. This could in turn reflect mechanisms responsible for seizure generation and propagation, respectively. Studies in animals have shown that seizures are characterized by bidirectional activity (Derchansky et al., 2006). Further strengthening this hypothesis, is our observation of a specific divergent/convergent "architecture" of epileptogenic networks during interictal periods as well, which is in agreement with the observation of Horstmann et al. that epileptic networks differ in their global characteristics from non-epileptic networks (Horstmann et al., 2010). This network architecture of highly interconnected nodes, or neuronal positive feedback loops, may play a leading role in generating and propagating ictal activity. Focal ictal onsets may be manifestations of altered or abnormal connectivity within the networks that comprise the epileptogenic zone. If true, targeted selective disruption or modulation of the network components could be used for prevention or termination of seizures, without the need for removing the entire network.

5. Conclusions

SdDTF analysis of effective connectivity for high frequency activity (70–175 Hz) in ictal, pre-ictal and interictal recordings may help estimate the epileptogenic zone during invasive monitoring in patients with focal ictal onsets. The nodes of epileptogenic networks may be identified by assessing the combined divergence and convergence of propagated high frequency activity, and the relative importance of these nodes to ictogenesis may be reflected by the intensity and stability of propagation. These nodes may potentially serve as more reliable indices of the ictal onset zone than regions indicated solely by the high frequency energy content of ictal activity, and perhaps more reliable than nodes for lower frequency activity propagation. The nodes of high frequency activity flows appear to be stable throughout interictal periods, potentially making it possible to predict the ictal onset zone using interictal recordings alone. Automatic SdDTF analysis could potentially assist clinicians in the preoperative evaluation of patients undergoing epilepsy surgery, which presently is based on visual inspection of as many as 128 channels. This could be especially beneficial for patients who do not develop seizures during hospital admission. Moreover, the ability of SdDTF analysis to reveal the most active nodes from the group of electrodes identified by clinicians as a seizure onset zone may help in planning for epilepsy surgery in patients for whom the seizure onset zone overlaps with or is immediately adjacent to brain regions crucial for language and motor function. This could in turn help improve surgical outcomes with respect to seizure control and avoidance of surgical complications. The phenomenon of divergence/convergence observed in this study may also add to our understanding of the “architecture” of epileptogenic networks, perhaps revealing neuronal feedforward and feedback loops that enhance synchronization and contribute to seizure generation and propagation.

Acknowledgments

Supported by: Epilepsy Foundation and by NINDS R01 NS40596 (Crone) and R01 NS48222 (Bergey) and R01 NS75020 (Jouny)

References

Adhikari BM, Epstein CM, Dhamala M. Localizing epileptic seizure onsets with Granger causality. Phys Rev E Stat Nonlin Soft Matter Phys. 2013; 88:030701. [PubMed: 24125204]

Baccala LA, Alvarenga MY, Sameshima K, Jorge CL, Castro LH. Graph theoretical characterization and tracking of the effective neural connectivity during episodes of mesial temporal epileptic seizure. J Integr Neurosci. 2004; 3:379–395. [PubMed: 15657975]

Baccala LA, Sameshima K. Partial directed coherence: a new concept in neural structure determination. Biol Cybern. 2001; 84:463–474. [PubMed: 11417058]

Bettus G, Wendling F, Guye M, Valton L, Regis J, Chauvel P, Bartolomei F. Enhanced EEG functional connectivity in mesial temporal lobe epilepsy. Epilepsy Res. 2008; 81:58–68. [PubMed: 18547787]

Blaker H. Confidence curves and improved exact confidence intervals for discrete distributions. Canadian Journal of Statistics. 2000; 28:783–798. correction 729, 681.

Boatman-Reich D, Franaszczuk PJ, Korzeniewska A, Caffo B, Ritzl EK, Colwell S, Crone NE. Quantifying auditory event-related responses in multichannel human intracranial recordings. Front Comput Neurosci. 2010; 4:4. [PubMed: 20428513]

Bower MR, Stead M, Meyer FB, Marsh WR, Worrell GA. Spatiotemporal neuronal correlates of seizure generation in focal epilepsy. Epilepsia. 2012; 53:807–816. [PubMed: 22352423]

Bragin A, Engel J Jr, Staba RJ. High-frequency oscillations in epileptic brain. Curr Opin Neurol. 2010; 23:151–156. [PubMed: 20160649]

Brazdil M, Halamek J, Jurak P, Daniel P, Kuba R, Chrastina J, Novak Z, Rektor I. Interictal high-frequency oscillations indicate seizure onset zone in patients with focal cortical dysplasia. Epilepsy Res. 2010; 90:28–32. [PubMed: 20362416]

Burns SP, Sritharan D, Jouny C, Bergey G, Crone N, Anderson WS, Sarma SV. A network analysis of the dynamics of seizure. Conf Proc IEEE Eng Med Biol Soc. 2012; 2012:4684–4687. [PubMed: 23366973]

Cervenka MC, Boatman-Reich DF, Ward J, Franaszczuk PJ, Crone NE. Language mapping in multilingual patients: electrocorticography and cortical stimulation during naming. Front Hum Neurosci. 2011a; 5:13. [PubMed: 21373361]

Cervenka MC, Corines J, Boatman-Reich DF, Eloyan A, Sheng X, Franaszczuk PJ, Crone NE. Electrocorticographic functional mapping identifies human cortex critical for auditory and visual naming. Neuroimage. 2013a; 69:267–276. [PubMed: 23274183]

Cervenka MC, Franaszczuk PJ, Crone NE, Hong B, Caffo BS, Bhatt P, Lenz FA, Boatman-Reich D. Reliability of early cortical auditory gamma-band responses. Clin Neurophysiol. 2013b; 124:70–82. [PubMed: 22771035]

Cervenka MC, Nagle S, Boatman-Reich D. Cortical high-gamma responses in auditory processing. Am J Audiol. 2011b; 20:171–180. [PubMed: 22158634]

Chavez M, Valencia M, Navarro V, Latora V, Martinerie J. Functional modularity of background activities in normal and epileptic brain networks. Phys Rev Lett. 2010; 104:118701. [PubMed: 20366507]

Derchansky M, Rokni D, Rick JT, Wennberg R, Bardakjian BL, Zhang L, Yarom Y, Carlen PL. Bidirectional multisite seizure propagation in the intact isolated hippocampus: the multifocality of the seizure “focus”. Neurobiol Dis. 2006; 23:312–328. [PubMed: 16815026]

Ding L, Worrell GA, Lagerlund TD, He B. Ictal source analysis: localization and imaging of causal interactions in humans. Neuroimage. 2007; 34:575–586. [PubMed: 17112748]

Ding M, Bressler SL, Yang W, Liang H. Short-window spectral analysis of cortical event-related potentials by adaptive multivariate autoregressive modeling: data preprocessing, model validation, and variability assessment. Biol Cybern. 2000; 83:35–45. [PubMed: 10933236]

Douw L, de Groot M, van Dellen E, Heimans JJ, Ronner HE, Stam CJ, Reijneveld JC. ‘Functional connectivity’ is a sensitive predictor of epilepsy diagnosis after the first seizure. PLoS One. 2010a; 5:e10839. [PubMed: 20520774]

Douw L, van Dellen E, de Groot M, Heimans JJ, Klein M, Stam CJ, Reijneveld JC. Epilepsy is related to theta band brain connectivity and network topology in brain tumor patients. BMC Neurosci. 2010b; 11:103. [PubMed: 20731854]

Dudek FE, Sutula TP. Epileptogenesis in the dentate gyrus: a critical perspective. Prog Brain Res. 2007; 163:755–773. [PubMed: 17765749]

Engel J Jr, Bragin A, Staba R, Mody I. High-frequency oscillations: what is normal and what is not? Epilepsia. 2009; 50:598–604. [PubMed: 19055491]

Engel, J, Jr. Seizures and Epilepsy. 2 ed. Oxford, New York: Oxford University Press; 2012.

Firpi H, Smart O, Worrell G, Marsh E, Dlugos D, Litt B. High-frequency oscillations detected in epileptic networks using swarmed neural-network features. Ann Biomed Eng. 2007; 35:1573–1584. [PubMed: 17541826]

Fisher RA. The Logic of Inductive Inference. Journal of the Royal Statistical Society. 1935; 98:39–82.

Franaszczuk PJ, Bergey GK. Application of the directed transfer function method to mesial and lateral onset temporal lobe seizures. Brain Topogr. 1998; 11:13–21. [PubMed: 9758388]

Franaszczuk PJ, Bergey GK, Kaminski MJ. Analysis of mesial temporal seizure onset and propagation using the directed transfer function method. Electroencephalogr Clin Neurophysiol. 1994; 91:413–427. [PubMed: 7529681]

Frei MG, Zaveri HP, Arthurs S, Bergey GK, Jouny CC, Lehnertz K, Gotman J, Osorio I, Netoff TI, Freeman WJ, Jefferys J, Worrell G, Quyen Mle V, Schiff SJ, Mormann F. Controversies in

epilepsy: debates held during the Fourth International Workshop on Seizure Prediction. Epilepsy Behav. 2010; 19:4–16. [PubMed: 20708976]

Friston KJ. Functional and effective connectivity in neuroimaging: A synthesis. Human Brain Mapping. 1994; 2:56–78.

Fujiwara H, Greiner HM, Lee KH, Holland-Bouley KD, Seo JH, Arthur T, Mangano FT, Leach JL, Rose DF. Resection of ictal high-frequency oscillations leads to favorable surgical outcome in pediatric epilepsy. Epilepsia. 2012; 53:1607–1617. [PubMed: 22905734]

Ge M, Jiang X, Bai Q, Yang S, Gusphyl J, Yan W. Application of the directed transfer function method to the study of the propagation of epilepsy neural information. Conf Proc IEEE Eng Med Biol Soc. 2007; 2007:3266–3269. [PubMed: 18002692]

Granger CWJ. Investigating causal relations by econometric models and cross-spectral methods. Econometrica. 1969; 37:424–438.

Horstmann MT, Bialonski S, Noennig N, Mai H, Prusseit J, Wellmer J, Hinrichs H, Lehnertz K. State dependent properties of epileptic brain networks: comparative graph-theoretical analyses of simultaneously recorded EEG and MEG. Clin Neurophysiol. 2010; 121:172–185. [PubMed: 20045375]

Jacobs J, Levan P, Chander R, Hall J, Dubeau F, Gotman J. Interictal high-frequency oscillations (80–500 Hz) are an indicator of seizure onset areas independent of spikes in the human epileptic brain. Epilepsia. 2008

Jacobs J, Staba R, Asano E, Otsubo H, Wu JY, Zijlmans M, Mohamed I, Kahane P, Dubeau F, Navarro V, Gotman J. High-frequency oscillations (HFOs) in clinical epilepsy. Prog Neurobiol. 2012; 98:302–315. [PubMed: 22480752]

Jacobs J, Zelmann R, Jirsch J, Chander R, Dubeau CE, Gotman J. High frequency oscillations (80–500 Hz) in the preictal period in patients with focal seizures. Epilepsia. 2009; 50:1780–1792. [PubMed: 19400871]

Jacobs J, Zijlmans M, Zelmann R, Chatillon CE, Hall J, Olivier A, Dubeau F, Gotman J. High-frequency electroencephalographic oscillations correlate with outcome of epilepsy surgery. Ann Neurol. 2010; 67:209–220. [PubMed: 20225281]

Jirsch JD, Urrestarazu E, LeVan P, Olivier A, Dubeau F, Gotman J. High-frequency oscillations during human focal seizures. Brain. 2006; 129:1593–1608. [PubMed: 16632553]

Jiruska P, Bragin A. High-frequency activity in experimental and clinical epileptic foci. Epilepsy Res. 2011; 97:300–307. [PubMed: 22024189]

Jiruska P, Powell AD, Chang WC, Jefferys JG. Electrographic high-frequency activity and epilepsy. Epilepsy Res. 2010; 89:60–65. [PubMed: 20031373]

Jouny CC, Adamolekun B, Franaszczuk PJ, Bergey GK. Intrinsic ictal dynamics at the seizure focus: effects of secondary generalization revealed by complexity measures. Epilepsia. 2007a; 48:297–304. [PubMed: 17295623]

Jouny CC, Afra P, Franaszczuk PJ, Bergey GK. Is high-frequency activity relevant to seizure onset localization. Epilepsia. 2007b; 48:199–200.

Jouny CC, Franaszczuk PJ, Bergey GK. Characterization of epileptic seizure dynamics using Gabor atom density. Clin Neurophysiol. 2003; 114:426–437. [PubMed: 12705423]

Jung YJ, Kang HC, Choi KO, Lee JS, Kim DS, Cho JH, Kim SH, Im CH, Kim HD. Localization of ictal onset zones in Lennox-Gastaut syndrome using directional connectivity analysis of intracranial electroencephalography. Seizure. 2011; 20:449–457. [PubMed: 21515079]

Kaminski MJ, Blinowska KJ. A new method of the description of the information flow in the brain structures. Biol Cybern. 1991; 65:203–210. [PubMed: 1912013]

Korzeniewska A, Crainiceanu CM, Kus R, Franaszczuk PJ, Crone NE. Dynamics of event-related causality in brain electrical activity. Hum Brain Mapp. 2008; 29:1170–1192. [PubMed: 17712784]

Korzeniewska, A.; Flinker, A.; Franaszczuk, PJ.; Lenz, FA.; Knight, RT.; NE; C. Dynamics of effective connectivity at high-gamma frequencies in large-scale human cortical networks during word production. In: SfN, editor. Neuroscience. San Diego: 2012a.

Korzeniewska, A.; Franaszczuk, PJ.; Cervenka, MC.; Jouny, CC.; Bergey, GK.; Crone, NE. Human epileptogenic networks are revealed by propagation of ictal and post-ictal high frequency activity (70–170 Hz); San Diego, CA. The American Epilepsy Society's Annual Meeting; 2012b.

Korzeniewska A, Franaszczuk PJ, Crainiceanu CM, Kus R, Crone NE. Dynamics of large-scale cortical interactions at high gamma frequencies during word production: event related causality (ERC) analysis of human electrocorticography (ECoG). Neuroimage. 2011; 56:2218–2237. [PubMed: 21419227]

Korzeniewska A, Jouny CC, Kus R, Bergey G, Crone NE, Franaszczuk PJ. Bidirectional propagation of high-frequency interictal and preictal activity (70–170 Hz) as an indicator of seizure foci. Epilepsia. 2009; 50:36.

Korzeniewska A, Manczak M, Kaminski M, Blinowska KJ, Kasicki S. Determination of information flow direction among brain structures by a modified directed transfer function (dDTF) method. J Neurosci Methods. 2003; 125:195–207. [PubMed: 12763246]

Lu Y, Yang L, Worrell GA, He B. Seizure source imaging by means of FINE spatio-temporal dipole localization and directed transfer function in partial epilepsy patients. Clin Neurophysiol. 2012; 123:1275–1283. [PubMed: 22172768]

Mallat S, Zhang Z. Matching pursuit with time-frequency dictionaries. IEEE Transactions on Signal Processing. 1993; 41:3397–3415.

Medvedev A, Willoughby JO. Autoregressive modeling of the EEG in systemic kainic acid-induced epileptogenesis. Int J Neurosci. 1999; 97:149–167. [PubMed: 10372644]

Modur PN, Zhang S, Vitaz TW. Ictal high-frequency oscillations in neocortical epilepsy: implications for seizure localization and surgical resection. Epilepsia. 2011; 52:1792–1801. [PubMed: 21762451]

Molenberghs GV, G. Models for discrete longitudinal data. Springer. 2005

Monto S, Vanhatalo S, Holmes MD, Palva JM. Epileptogenic neocortical networks are revealed by abnormal temporal dynamics in seizure-free subdural EEG. Cereb Cortex. 2007; 17:1386–1393. [PubMed: 16908492]

Morgan RJ, Soltesz I. Nonrandom connectivity of the epileptic dentate gyrus predicts a major role for neuronal hubs in seizures. Proc Natl Acad Sci U S A. 2008; 105:6179–6184. [PubMed: 18375756]

Mullen T, Acar ZA, Worrell G, Makeig S. Modeling cortical source dynamics and interactions during seizure. Conf Proc IEEE Eng Med Biol Soc. 2011; 2011:1411–1414. [PubMed: 22254582]

Nair DR, Mohamed A, Burgess R, Luders H. A critical review of the different conceptual hypotheses framing human focal epilepsy. Epileptic Disord. 2004; 6:77–83. [PubMed: 15246951]

Nariai H, Matsuzaki N, Juhasz C, Nagasawa T, Sood S, Chugani HT, Asano E. Ictal high-frequency oscillations at 80–200 Hz coupled with delta phase in epileptic spasms. Epilepsia. 2011a; 52:e130–e134. [PubMed: 21972918]

Nariai H, Nagasawa T, Juhasz C, Sood S, Chugani HT, Asano E. Statistical mapping of ictal high-frequency oscillations in epileptic spasms. Epilepsia. 2011b; 52:63–74. [PubMed: 21087245]

Ochi A, Otsubo H, Donner EJ, Elliott I, Iwata R, Funaki T, Akizuki Y, Akiyama T, Imai K, Rutka JT, Snead OC 3rd. Dynamic changes of ictal high-frequency oscillations in neocortical epilepsy: using multiple band frequency analysis. Epilepsia. 2007; 48:286–296. [PubMed: 17295622]

Ortega GJ, Sola RG, Pastor J. Complex network analysis of human ECoG data. Neurosci Lett. 2008; 447:129–133. [PubMed: 18848970]

Perucca P, Dubeau F, Gotman J. Intracranial electroencephalographic seizure-onset patterns: effect of underlying pathology. Brain. 2014; 137:183–196. [PubMed: 24176980]

Rampp S, Stefan H. Fast activity as a surrogate marker of epileptic network function? Clin Neurophysiol. 2006; 117:2111–2117. [PubMed: 16843722]

Rodin E, Constantino T, Rampp S, Modur P. Seizure onset determination. J Clin Neurophysiol. 2009; 26:1–12. [PubMed: 19151615]

Sameshima K, Baccala LA. Using partial directed coherence to describe neuronal ensemble interactions. J Neurosci Methods. 1999; 94:93–103. [PubMed: 10638818]

Sanchez Fernandez I, Abend NS, Arndt DH, Carpenter JL, Chapman KE, Cornett KM, Dlugos DJ, Gallentine WB, Giza CC, Goldstein JL, Hahn CD, Lerner JT, Matsumoto JH, McBain K, Nash KB, Payne E, Sanchez SM, Williams K, Loddenkemper T. Electrographic seizures after convulsive status epilepticus in children and young adults: a retrospective multicenter study. J Pediatr. 2014; 164:339–346. e331–e332. [PubMed: 24161223]

Schevon CA, Weiss SA, McKhann G Jr, Goodman RR, Yuste R, Emerson RG, Trevelyan AJ. Evidence of an inhibitory restraint of seizure activity in humans. Nat Commun. 2012; 3:1060. [PubMed: 22968706]

Sinai A, Bowers CW, Crainiceanu CM, Boatman D, Gordon B, Lesser RP, Lenz FA, Crone NE. Electrocorticographic high gamma activity versus electrical cortical stimulation mapping of naming. Brain. 2005; 128:1556–1570. [PubMed: 15817517]

Sporns O. Brain connectivity. Scholarpedia. 2007:4695.

Takahashi DY, Baccala LA, Yang HM. Connectivity inference between neural structures via partial directed coherence. Journal of Applied Statistics. 2007; 34:1255–1269.

Traub RD, Wong RK. Cellular mechanism of neuronal synchronization in epilepsy. Science. 1982; 216:745–747. [PubMed: 7079735]

Uhlhaas PJ, Singer W. Neural synchrony in brain disorders: relevance for cognitive dysfunctions and pathophysiology. Neuron. 2006; 52:155–168. [PubMed: 17015233]

van Diessen E, Diederen SJ, Braun KP, Jansen FE, Stam CJ. Functional and structural brain networks in epilepsy: What have we learned? Epilepsia. 2013

van Mierlo P, Carrette E, Hallez H, Raedt R, Meurs A, Vandenberghe S, Van Roost D, Boon P, Staelens S, Vonck K. Ictal-onset localization through connectivity analysis of intracranial EEG signals in patients with refractory epilepsy. Epilepsia. 2013

van Mierlo P, Carrette E, Hallez H, Vonck K, Van Roost D, Boon P, Staelens S. Accurate epileptogenic focus localization through time-variant functional connectivity analysis of intracranial electroencephalographic signals. Neuroimage. 2011; 56:1122–1133. [PubMed: 21316472]

Varotto G, Tassi L, Franceschetti S, Spreafico R, Panzica F. Epileptogenic networks of type II focal cortical dysplasia: a stereo-EEG study. Neuroimage. 2012a; 61:591–598. [PubMed: 22510255]

Varotto G, Visani E, Canafoglia L, Franceschetti S, Avanzini G, Panzica F. Enhanced frontocentral EEG connectivity in photosensitive generalized epilepsies: a partial directed coherence study. Epilepsia. 2012b; 53:359–367. [PubMed: 22191664]

Warren CP, Hu S, Stead M, Brinkmann BH, Bower MR, Worrell GA. Synchrony in Normal and Focal Epileptic Brain: The Seizure Onset Zone is Functionally Disconnected. J Neurophysiol. 2010

Wieser HG, Blume WT, Fish D, Goldensohn E, Hufnagel A, King D, Sperling MR, Luders H, Pedley TA. ILAE Commission Report. Proposal for a new classification of outcome with respect to epileptic seizures following epilepsy surgery. Epilepsia. 2001; 42:282–286. [PubMed: 11240604]

Wilke C, Ding L, He B. Estimation of time-varying connectivity patterns through the use of an adaptive directed transfer function. IEEE Trans Biomed Eng. 2008; 55:2557–2564. [PubMed: 18990625]

Wilke C, van Drongelen W, Kohrman M, He B. Identification of epileptogenic foci from causal analysis of ECoG interictal spike activity. Clin Neurophysiol. 2009a; 120:1449–1456. [PubMed: 19616474]

Wilke C, van Drongelen W, Kohrman M, He B. Neocortical seizure foci localization by means of a directed transfer function method. Epilepsia. 2010; 51:564–572. [PubMed: 19817817]

Wilke C, Worrell G, He B. Graph analysis of epileptogenic networks in human partial epilepsy. Epilepsia. 2011; 52:84–93. [PubMed: 21126244]

Wilke C, Worrell GA, He B. Analysis of epileptogenic network properties during ictal activity. Conf Proc IEEE Eng Med Biol Soc. 2009b; 2009:2220–2223. [PubMed: 19964953]

Worrell GA, Gardner AB, Stead SM, Hu S, Goerss S, Cascino GJ, Meyer FB, Marsh R, Litt B. High-frequency oscillations in human temporal lobe: simultaneous microwire and clinical macroelectrode recordings. Brain. 2008; 131:928–937. [PubMed: 18263625]

Worrell GA, Parish L, Cranstoun SD, Jonas R, Baltuch G, Litt B. High-frequency oscillations and seizure generation in neocortical epilepsy. Brain. 2004; 127:1496–1506. [PubMed: 15155522]

Yaari Y, Beck H. "Epileptic neurons" in temporal lobe epilepsy. Brain Pathol. 2002; 12:234–239. [PubMed: 11958377]

Zijlmans M, Jacobs J, Kahn YU, Zelmann R, Dubeau F, Gotman J. Ictal and interictal high frequency oscillations in patients with focal epilepsy. Clin Neurophysiol. 2011; 122:664–671. [PubMed: 21030302]

Zijlmans M, Jacobs J, Zelmann R, Dubeau F, Gotman J. High-frequency oscillations mirror disease activity in patients with epilepsy. Neurology. 2009; 72:979–986. [PubMed: 19289737]

Zijlmans M, Jiruska P, Zelmann R, Leijten FS, Jefferys JG, Gotman J. High-frequency oscillations as a new biomarker in epilepsy. Ann Neurol. 2012; 71:169–178. [PubMed: 22367988]

Highlights

- high frequency activity propagation identifies the seizure onset zone
- patterns of propagation during seizures are recapitulated in interictal recordings
- patterns of propagation differ for seizures with focal vs. regional onset
- epilepsy is associated with divergent/convergent architecture of cortical networks

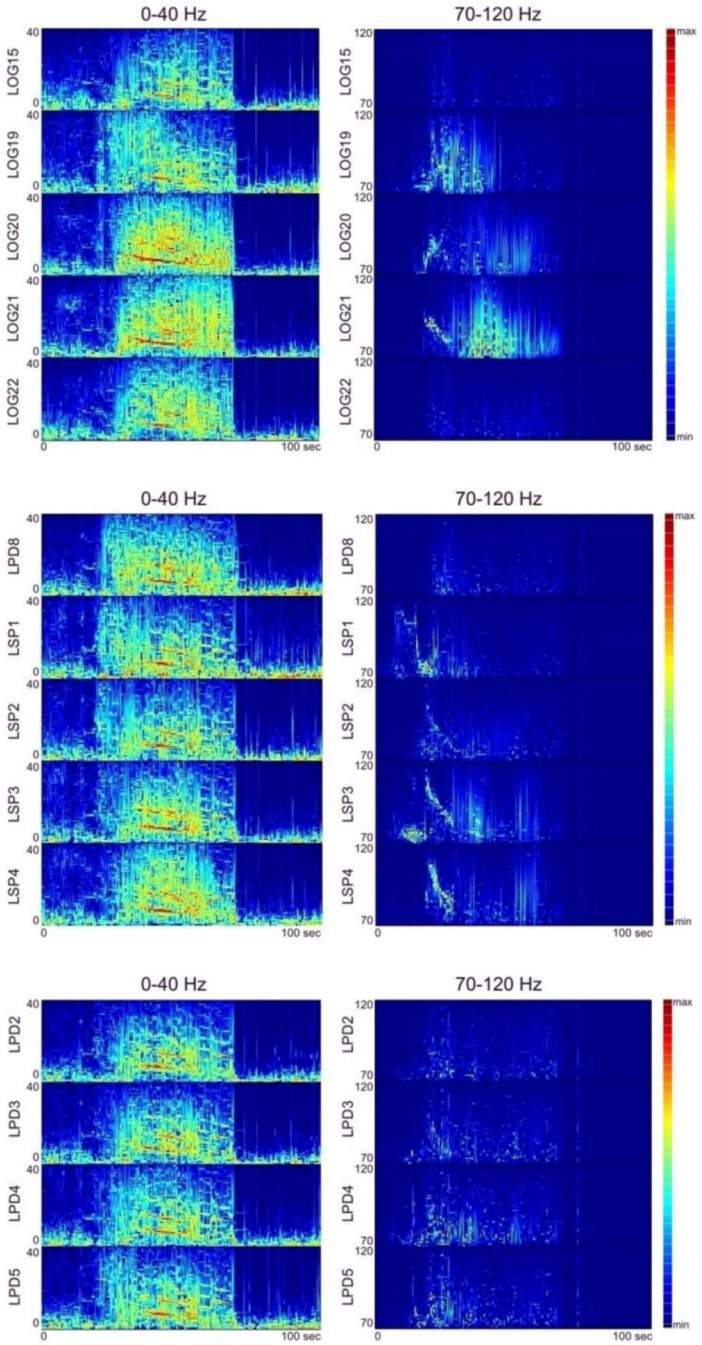

Fig. 1.

Changes in energy, in the time-frequency domain, for lower (0–40 Hz, left panels), and high frequency (70–120 Hz, right panels) components of ictal activity of several neighboring recording sites in Patient #1. Each plot depicts ECoG signal energy calculated using a matching pursuit (MP) algorithm of signal decomposition for lower frequencies 0–40 Hz (left panel) and for high frequencies (70–120 Hz, right panel), with a red to blue color spectrum where red is the maximum increase in energy and blue is no (zero) increase in energy compared to the pre-ictal baseline interval. The horizontal axis of each plot shows

the time scale in seconds (starting from seizure onset at time zero, as identified by epileptologists); vertical axis - frequency scale in Hz.

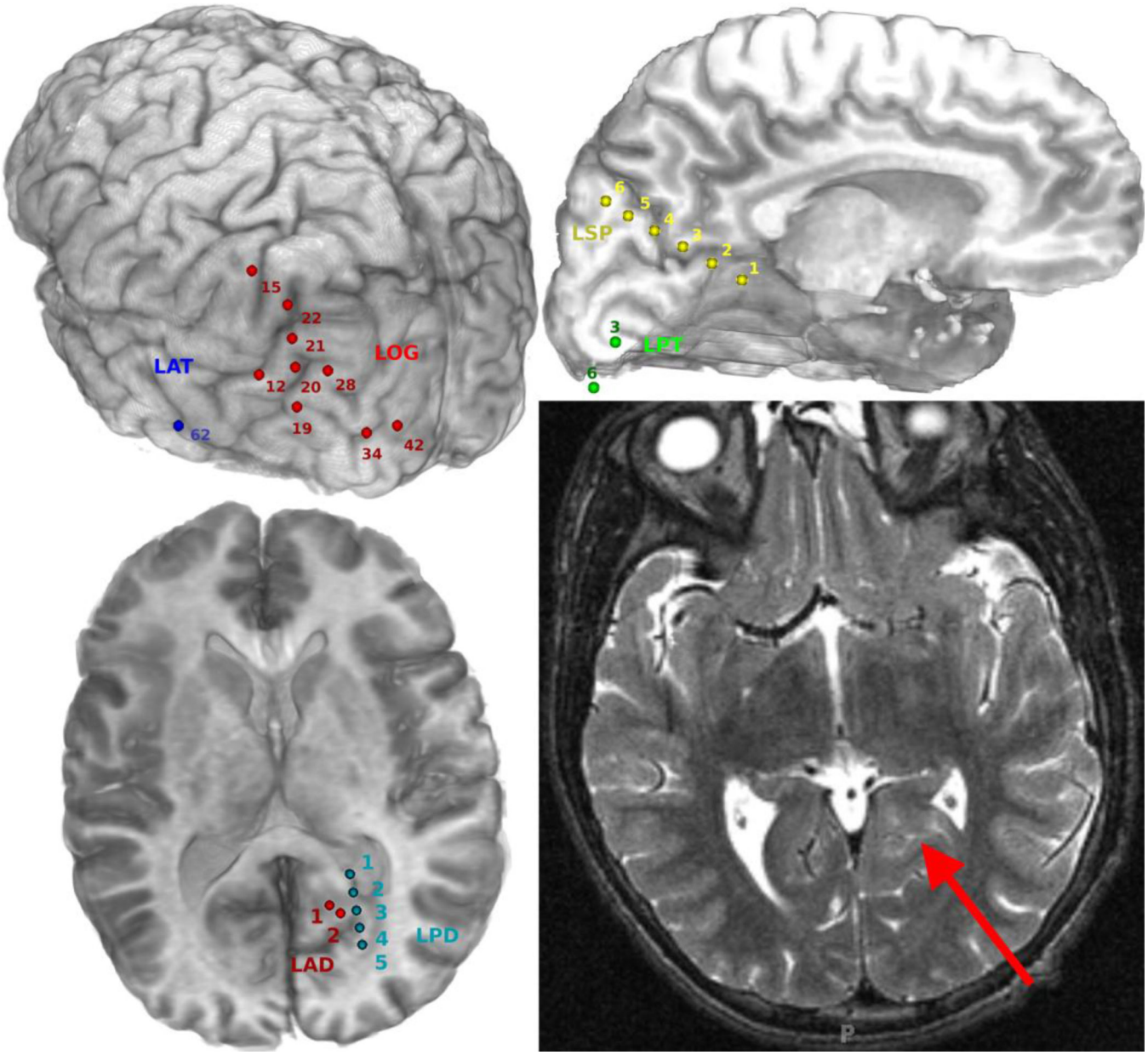

Fig. 2.

Reconstructions of the implanted electrodes in Patient #1, second admission (top left - left posterior oblique view of strip and grid electrodes, top right - left interhemispheric view of strip electrodes, bottom left - axial view of depth electrodes) and an axial T2-weighted MRI depicting a left mesial occipital lesion identified on pre-operative MRI (bottom-right).

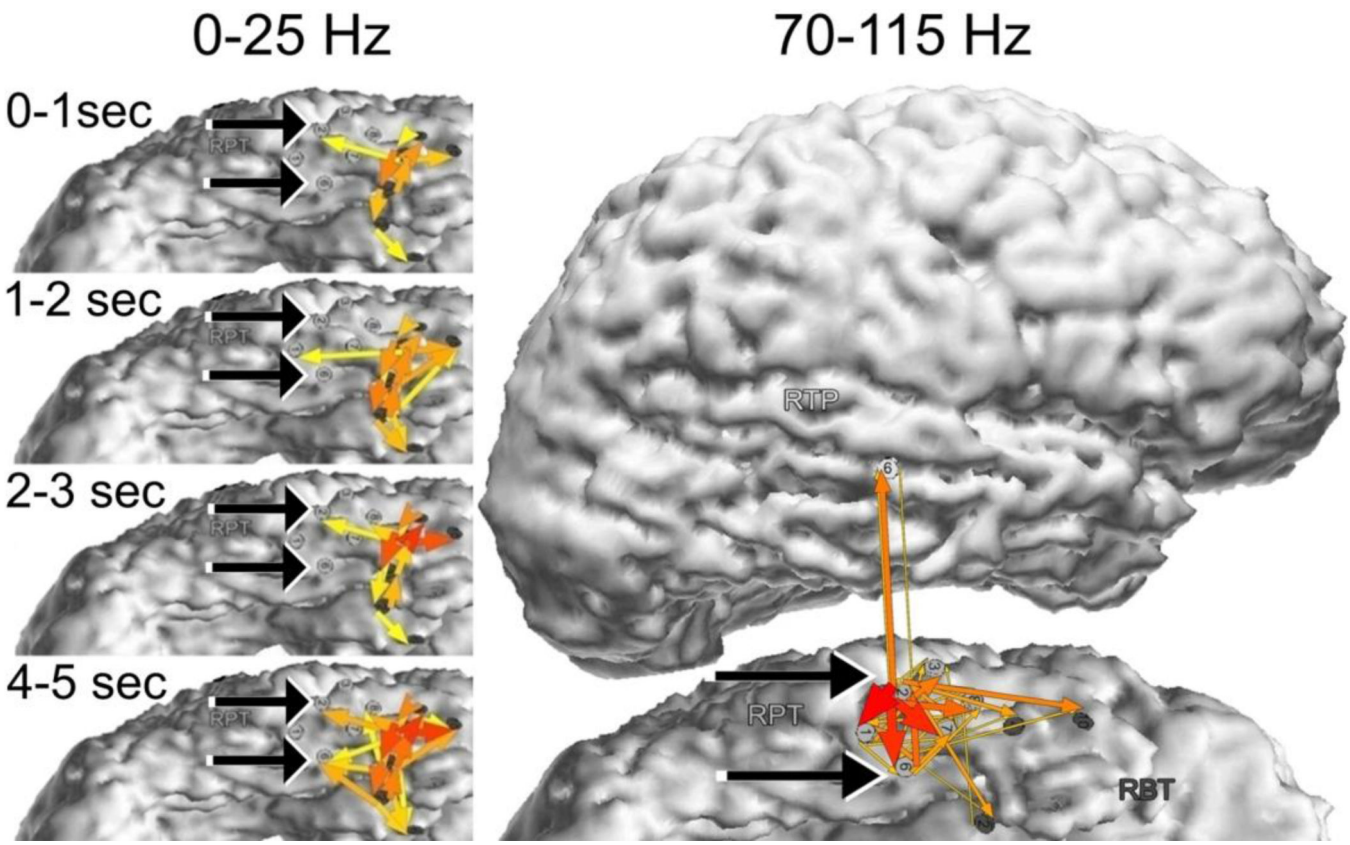

Fig. 3.

Integrals of SdDTF for lower and high frequency ictal propagations for Patient #2. Red-yellow arrows indicate the directions and intensities of the activity propagation. The width and color of each arrow represent values of SdDTF integrated over frequency and time. Two black arrows indicate electrodes of the epileptogenic zone (RPT2-RPT6) identified by epileptologists. Left panel - integrals of SdDTF for low frequency (0–25 Hz) ictal propagations calculated for consecutive seconds of ictal periods. Right panel - integrals of SdDTF for high frequency (70–115 Hz) ictal propagations calculated for whole ictal period.

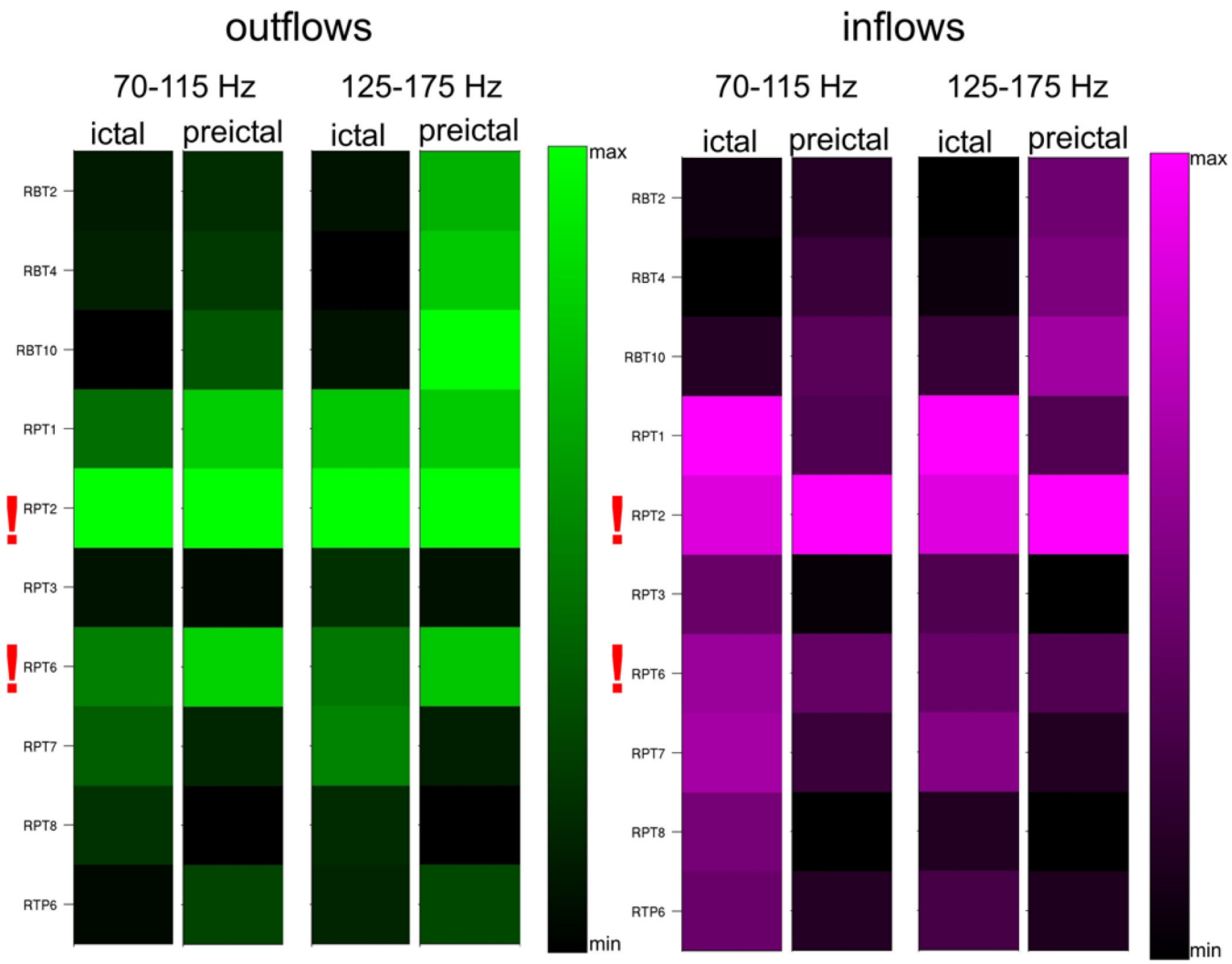

Fig. 4.

Averages of SdDTF for propagations between the site of ictal onset and all other recording sites, for the two frequency ranges 70–115 Hz and 125–175 Hz, during ictal and preictal periods in Patient #2. Each column shows average of SdDTFs for propagations *from* the site indicated at the left to all other recording sites (outflowing, green-black, left panel), and *to* the site indicated at the left from all other recording sites (inflowing, purple-black, right panel). The highest magnitudes indicate the largest outflows (the brightest green), or the largest inflows (brightest purple). Electrodes of the epileptogenic zone (RPT2, RPT6) identified by epileptologists, are marked with red exclamation marks. The color-scale is normalized from minimum to maximum averaged value of SdDTF, which allows for comparisons of different frequency ranges, and inter-, pre-, and ictal periods.

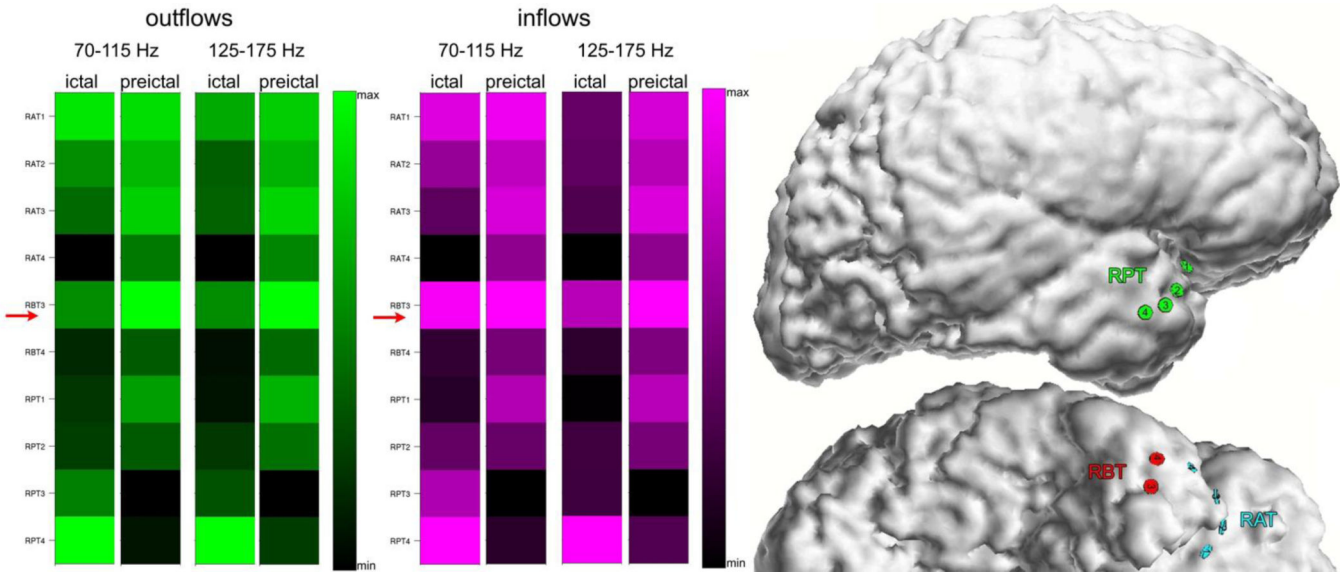

Fig. 5.

Averages of SdDTF for propagations between the site of ictal onset and all other recording sites, for two frequency ranges of 70–115 Hz and 125–175 Hz, during ictal and preictal periods for Patient #3. Color conventions and organization of the figure are as in Fig. 4. The right panel shows a right lateral and basal view of the brain with electrode positions depicted.

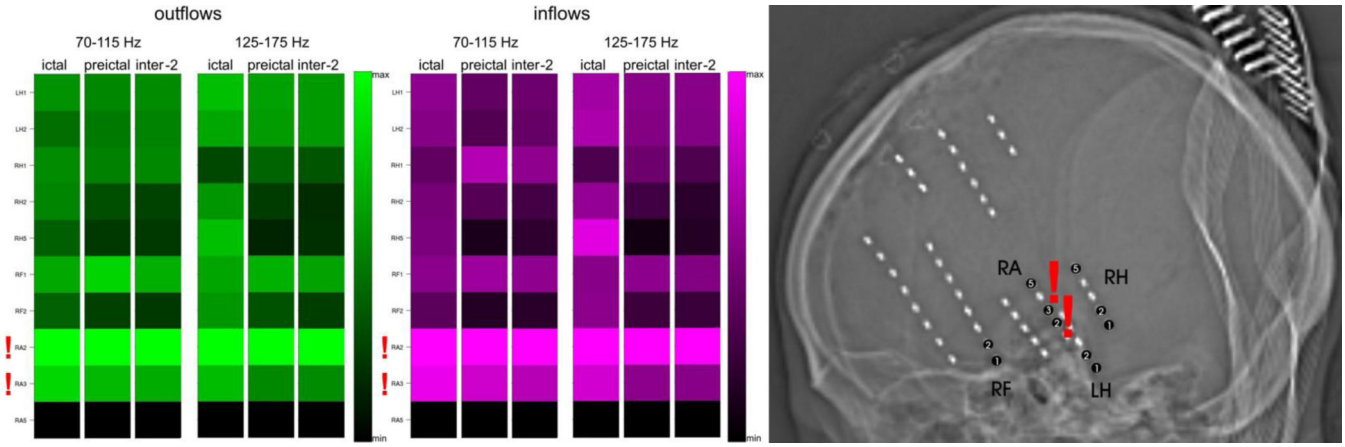

Fig. 6.

Averages of SdDTF for propagations between the site of ictal onset and all other recording sites, for two frequency ranges of 70–115 Hz and 125–175 Hz, during ictal, preictal, and interictal periods for Patient #4. Organization of the figure is as in Fig. 4. The right panel shows placement of depth electrodes by skull X-ray.

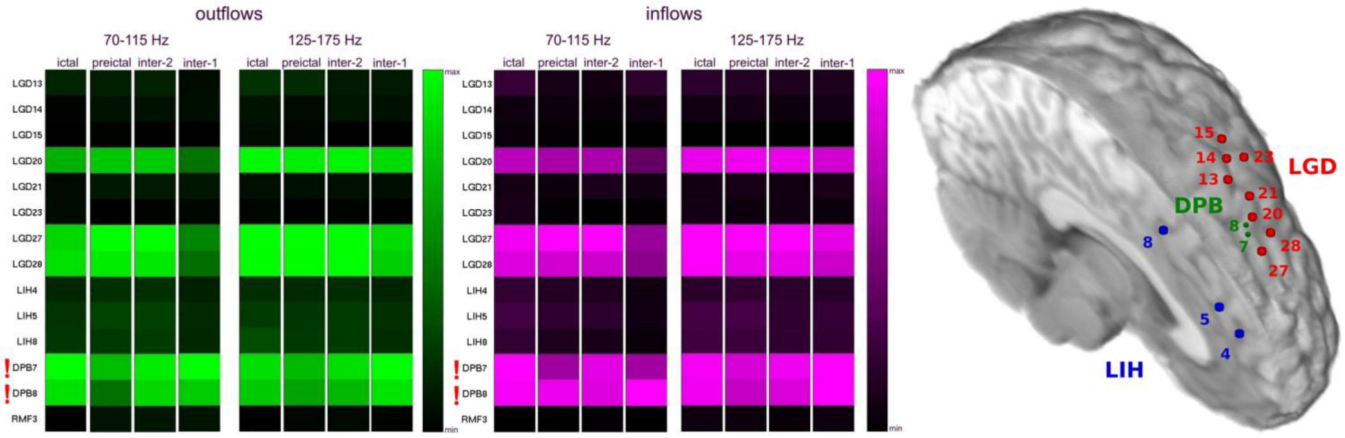

Fig. 7.

Averages of SdDTF for propagations between the site of ictal onset and all other recording sites, for two frequency ranges of 70–115 Hz and 125–175 Hz, during ictal, preictal, and interictal periods for Patient #5. Organization of the figure is as in Fig. 4. The right panel depicts a superior oblique interhemispheric view of the left hemisphere showing electrode positions.

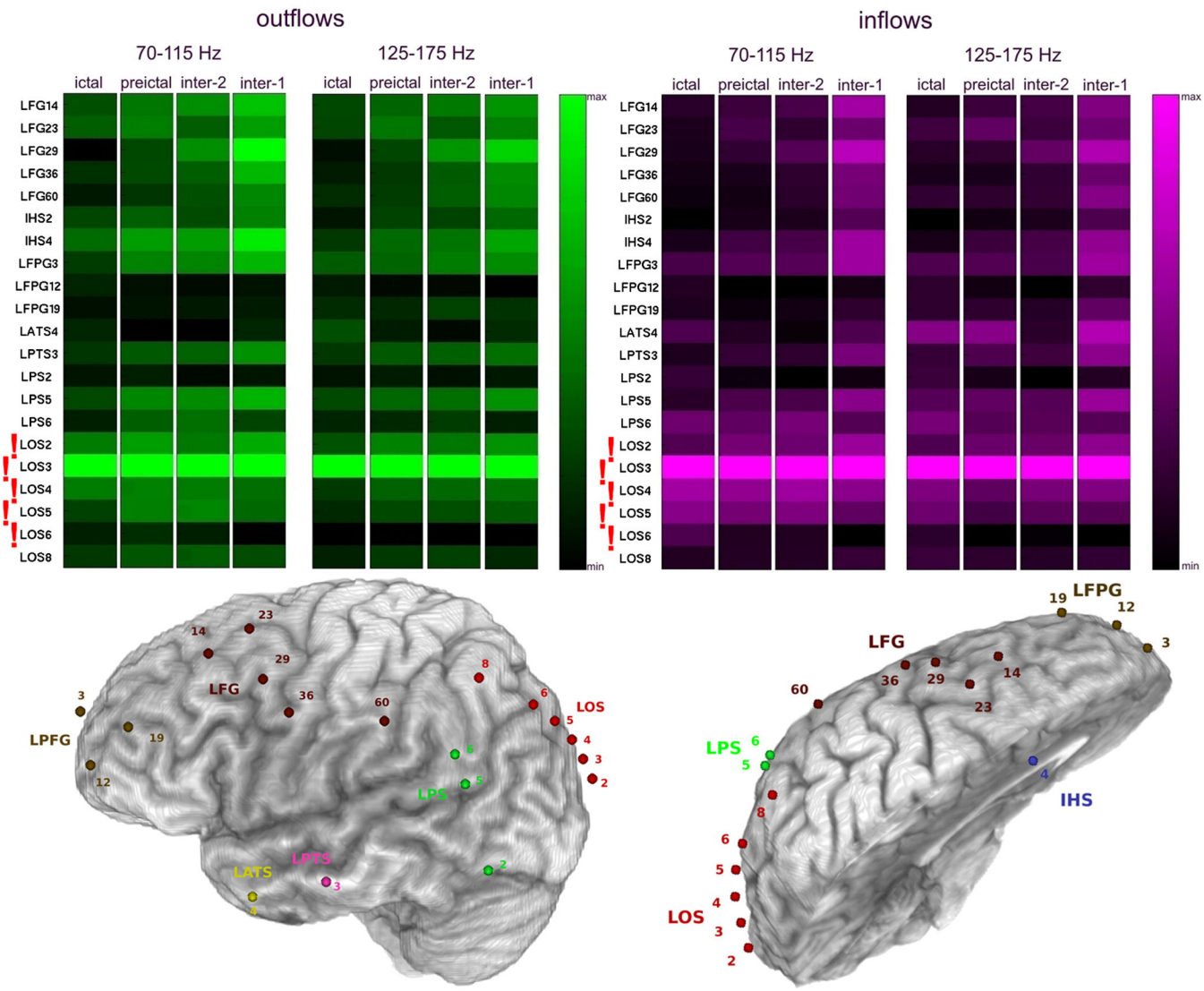

Fig. 8.

Averages of SdDTF for propagations between the site of ictal onset and all other recording sites, for two frequency ranges of 70–115 Hz and 125–175 Hz, during ictal, preictal, and interictal periods for the 1st admission for Patient #1. Organization of the figure is as in Fig. 4. The bottom panel depicts a left lateral (left) and superior oblique interhemispheric (right) view of the left hemisphere with electrode positions shown.

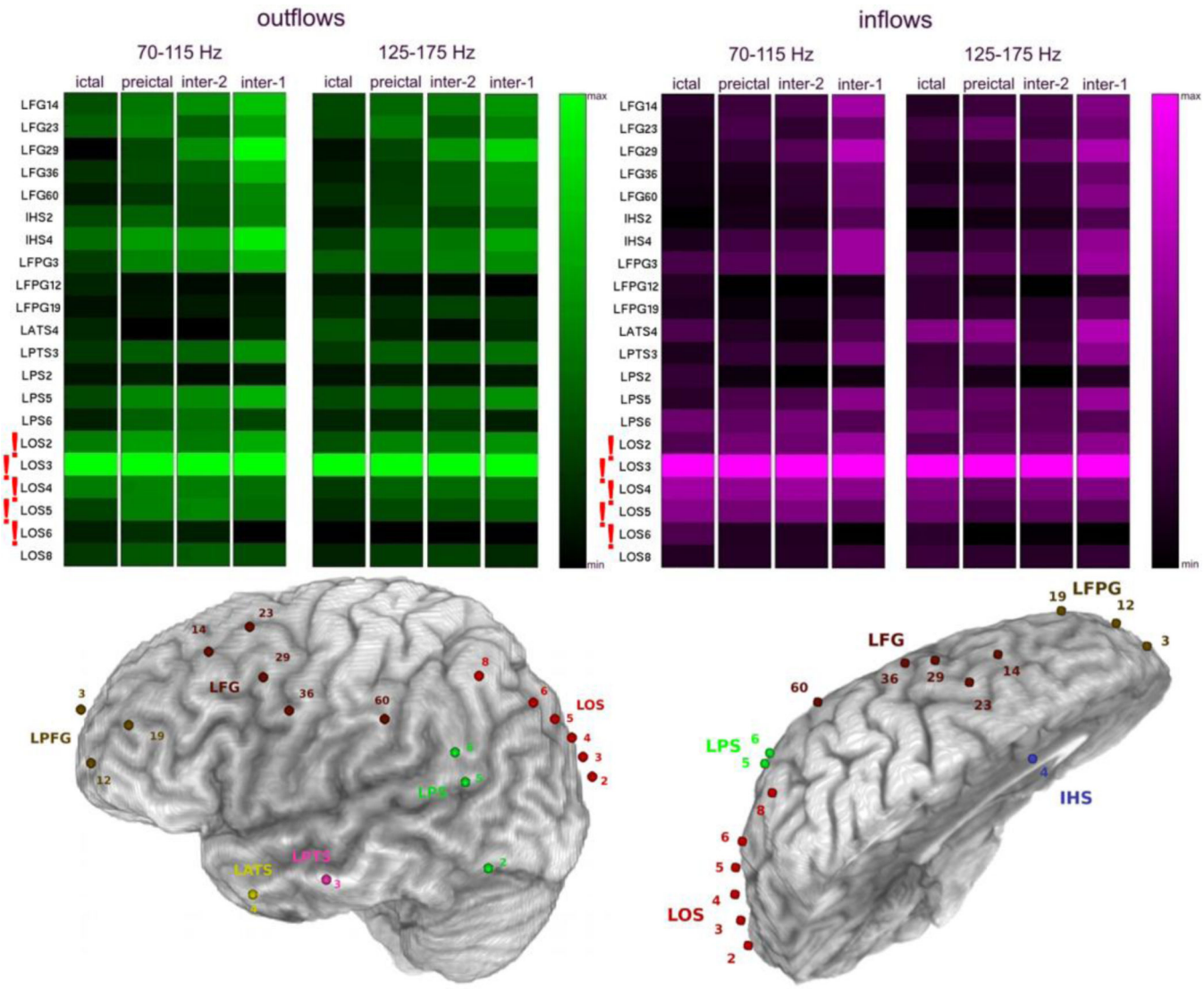

Fig. 9.

Averages of SdDTF for propagations between the site of ictal onset and all other recording sites, for lower frequency 0–40 Hz, during ictal, preictal, and interictal periods for the 1st admission for Patient #1. Organization of the figure is as in Fig. 4.

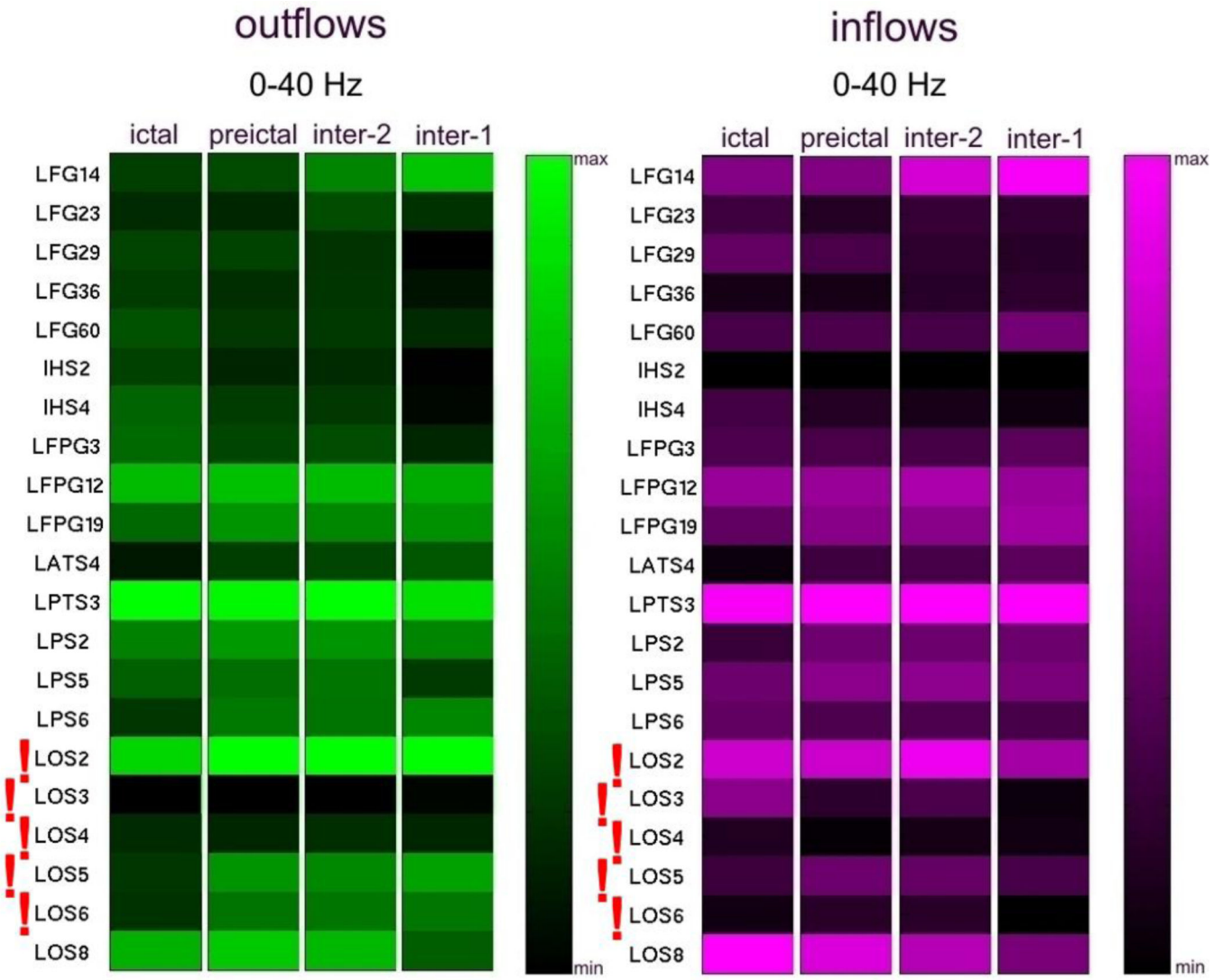

Fig. 10.

Averages of SdDTF for propagations between the site of ictal onset and all other recording sites, for two frequency ranges of 70–115 Hz and 125–175 Hz, during ictal, preictal, and interictal periods for 2nd admission of Patient #1. Organization of the figure is as in Fig. 4. Electrode positions are depicted in Figure 2.

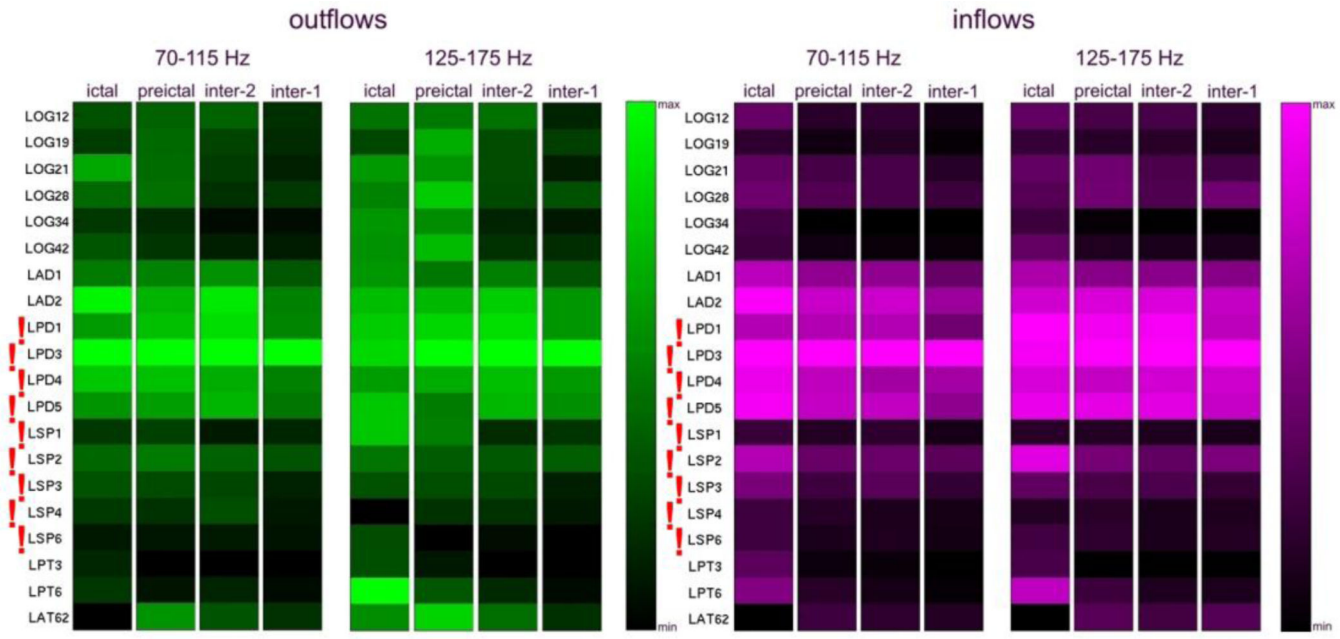

Fig. 11.

Averages of SdDTF for propagations between the site of ictal onset and all other recording sites, for lower frequency 0–40 Hz, during ictal, preictal, and interictal periods for 2nd admission of Patient #1. Organization of the figure is as in Fig. 4.

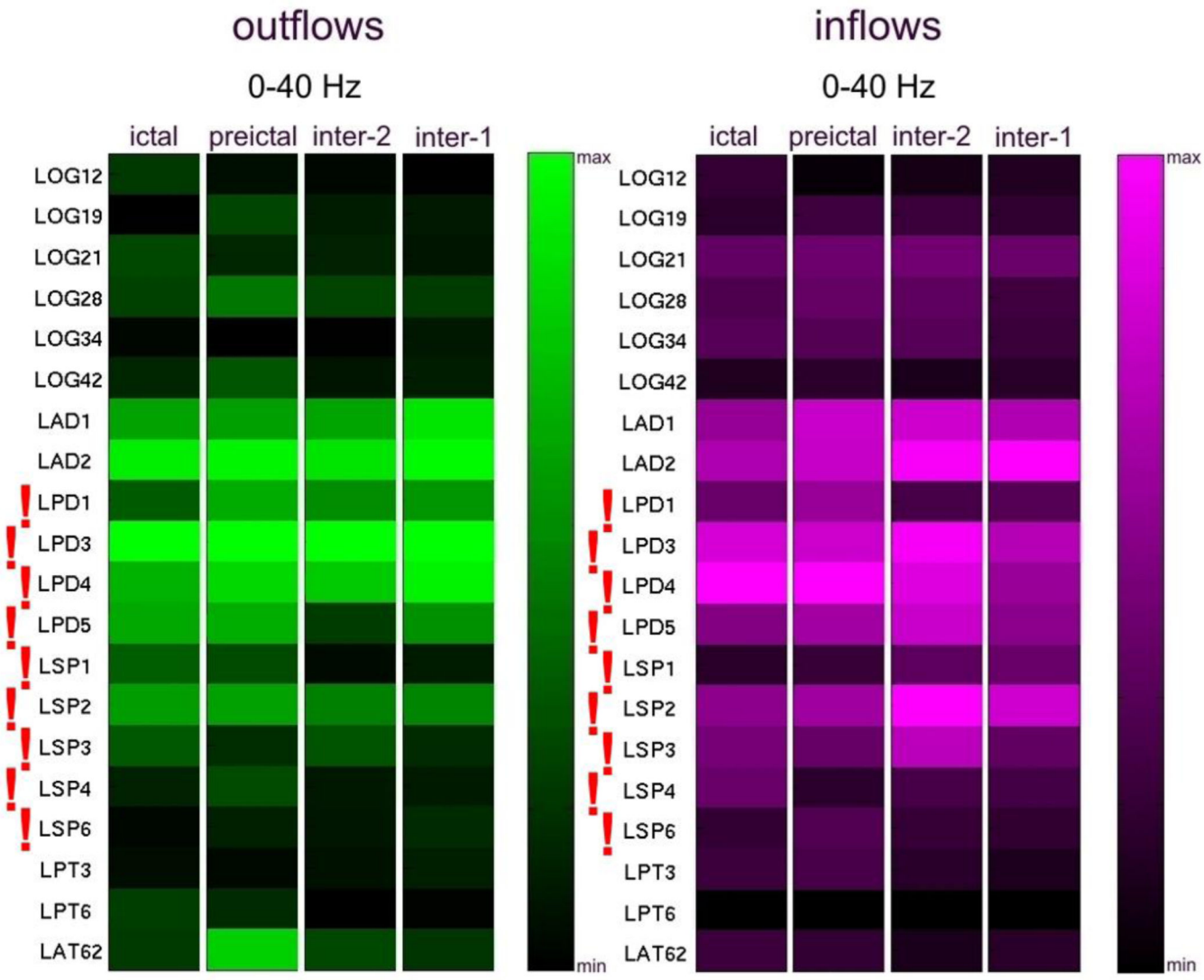

Fig. 12.

Averages of SdDTF for propagations between the site of ictal onset and all other recording sites, for two frequency ranges of 70–115 Hz and 125–175 Hz, during ictal, preictal, and interictal periods for Patient #6. Organization of the figure is as in Fig. 4. The center panel (left) shows an inferior left oblique view of the left hemisphere with electrode positions and (right) an axial T2 FLAIR MRI of the infiltrating left temporal lesion. The bottom panel (left) is a coronal view of the depth electrode positions and interhemispheric view with coronal cross sections through the planes traversing the paths of the depth electrodes.

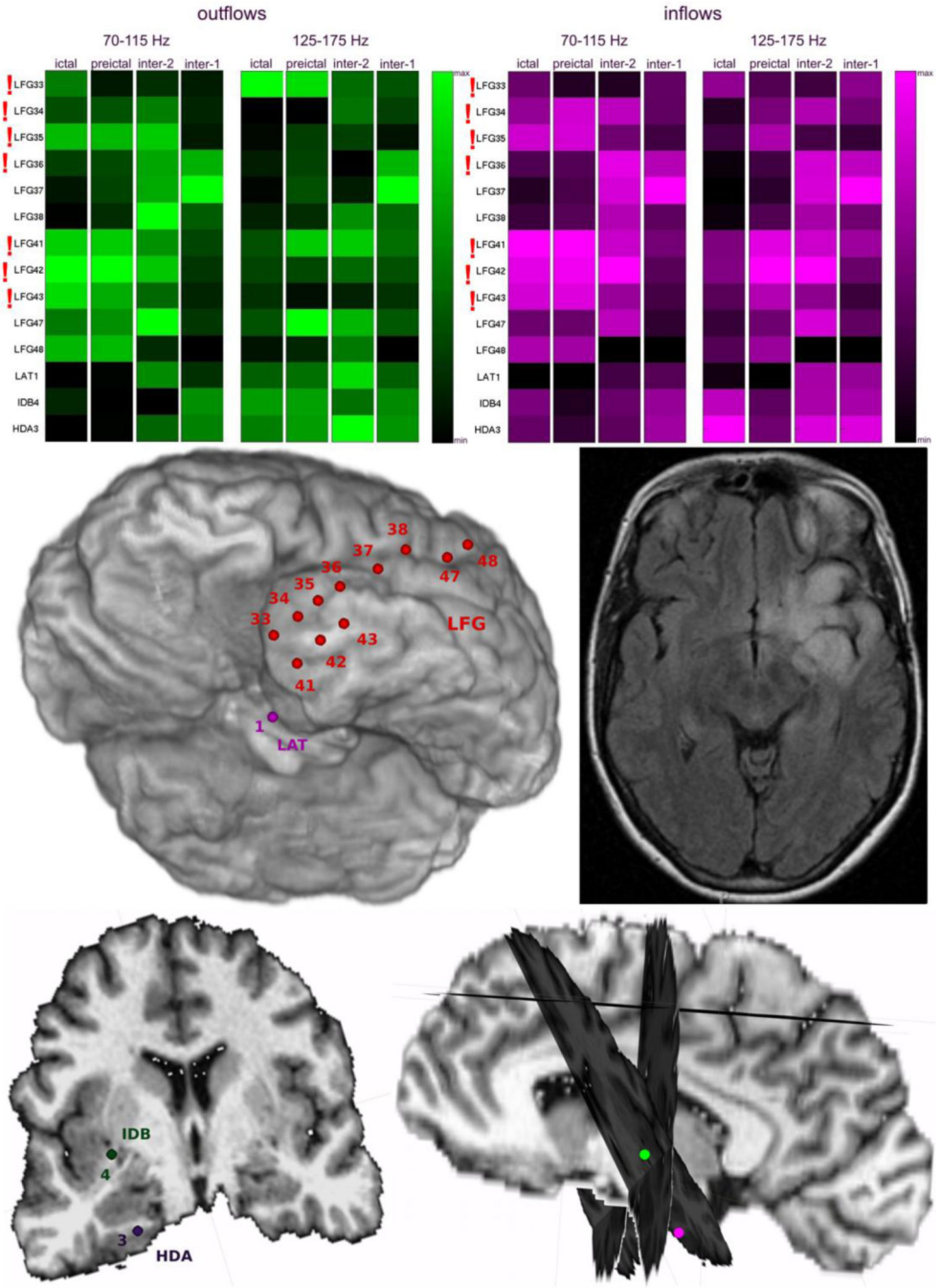

Fig. 13.

The mean value of the transformed averaged flows (MTAF) of high frequency activity propagation from and into each recording site, calculated for ictal, preictal, and interictal periods, for both ranges of high frequency, for each patient. Horizontal axis - recording sites, vertical axis - the degree of dominance.

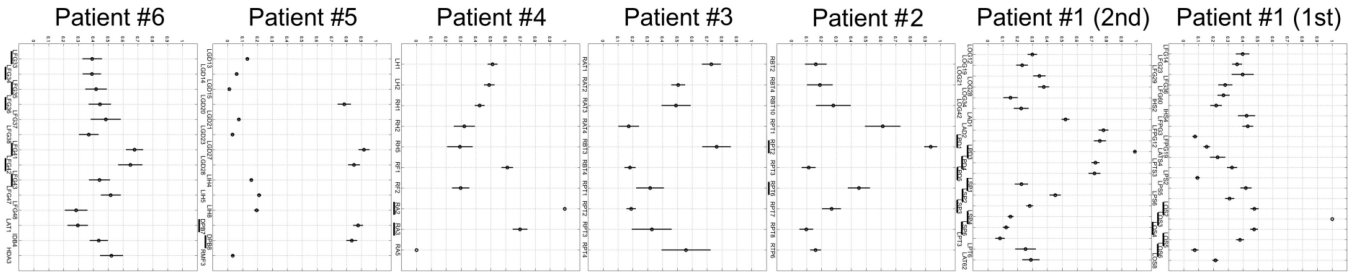

Fig. 14.

The mean value of the transformed averaged flows (MTAF) of high frequency activity propagation from and into each recording site, calculated for interictal periods, for both ranges of high frequency, in patients for whom the interictal intervals were available (not all interictal segments were saved for review in all patients). Horizontal axis - recording sites, vertical axis - the degree of dominance.

Table 1

The percentage of electrodes revealing significant increases in energy of ictal activity, as compared to energy of preictal activity, for frequency ranges 0–40 Hz, 75–115 Hz, and 125–175 Hz, for each patient diagnosed with focal, but not widely distributed ictal onset. The numbers in parentheses represent the ratio of electrodes revealing significant increases in energy of ictal activity to the total number of electrodes used in the analysis.

Patient # and type of electrodes	Number of seizures	0–40 Hz	75–115 Hz	125–175 Hz	Seizure onset zone identified by clinicians (electrodes)
#1 (1st admission) only grids	7	43% (48/112)	17% (19/112)	39% (44/112)	LOS2- LOS6 ictal activity in all frequency ranges
#1 2nd admission grids & depths	4	100% (87/87)	63% (55/87)	44% (38/87)	LPD1- LPD5, LSP1-LSP5 ictal activity in all frequency ranges
#2 only grids	86	100% (65/65)	45% (29/65)	45% (29/65)	RPT2, RPT6 ictal activity in all frequency ranges
#4 only depths	5	93% (25/27)	85% (23/27)	100% (27/27)	RA2-RA3 ictal activity in all frequency ranges
#5 grids & depths	9	15% (18/119)	2% (3/119)	8% (9/119)	DPB6-DPB8 ictal activity in all frequency ranges

Table 2

Recording sites identified as the ictal onset zone by epileptologists vs. those indicated by SdDTF analysis of propagation of high frequency activity.

Patient	**Seizure onset type**	**Number of seizures**	**Onset zone indicated by epileptologists**	**Onset zone indicated by high frequency propagation MTAF > 0.8 (ictal, preictal, inter-2, inter-1)**	**Onset zone indicated by high frequency propagation MTAF > 0.8 (inter-2)**	**Onset zone indicated by high frequency propagation MTAF > 0.8 (inter-1)**	**Surgical pathology Post-op outcome Duration follow up**
Patient #1 (1st admission)	focal	7	LOS2-LOS6	LOS3	LOS3	LOS3	no surgery N/A N/A
Patient #1 (2nd admission)	focal	4	LPD1-LPD5*, LSP1-LSP5*	LPD3*	LPD1*, LPD3*, LAD2*	LPD3*	DNET ILAE Class 1 3 years
Patient #2	focal	86	RPT2*, RPT6*	RPT2*	N/A	N/A	MTS ILAE Class 1 9 years
Patient #3	widely distributed	5	RAT1-RAT4*, RBT1-RBT4*, RPT1-RPT4*	NONE (highest - RAT1*, RBT3*)	N/A	N/A	MTS ILAE Class 1 5 years
Patient #4	focal	5	RA2-RA3*	RA2*	RA2*	N/A	MTS ILAE Class 1 7 years
Patient #5	focal	9	DPB6-DPB8*	DPB7*, DPB8*, LGD27*, LGD28*	DPB7*, DPB8*, LGD20* LGD27*, LGD28*	DPB7*, DPB8*,	cortical dysgenesis ILAE Class 1 4 years
Patient #6	widely distributed	3	LFG33-LFG36*, LFG41-LFG43*	NONE (highest - LFG41*, LFG42*)	LFG47	LFG37	oligodendroglioma ILAE Class 5 4 years

*Asterix indicates electrodes recording the tissue that was ultimately resected.

MP - matching pursuit

SdDTF - short-time direct directed transform function

Surgical outcome according to 2001 ILAE classification (Wieser et al., 2001).

Table 3

Number of electrodes identified by epileptologists as the ictal onset zone, and indicated by MTAF > 0.8.

Patient	Number of electrodes within the onset zone identified by epileptologists	Number of electrodes indicated by high frequency propagation overlapping with clinical diagnosis	Number of electrodes indicated by high frequency propagation non-overlapping with clinical diagnosis
Patient #1 (1st admission)	5	1	0
Patient #1 (2nd admission)	10	1	0
Patient #2	2	1	0
Patient #4	2	1	0
Patient #5	3	2	2

MP - matching pursuit

SdDTF - short-time direct directed transform function